MASTER'S DEGREE THESIS

Master of Science in Advanced Mathematics and Mathematical Engineering

Title: Warmer temperatures and their effect on East-African malaria

Author: Marta Pardo Araujo

Advisor: J. Tomás Lázaro Ochoa and David Alonso Giménez

Department: Dynamical systems

Academic year: 2019-2020

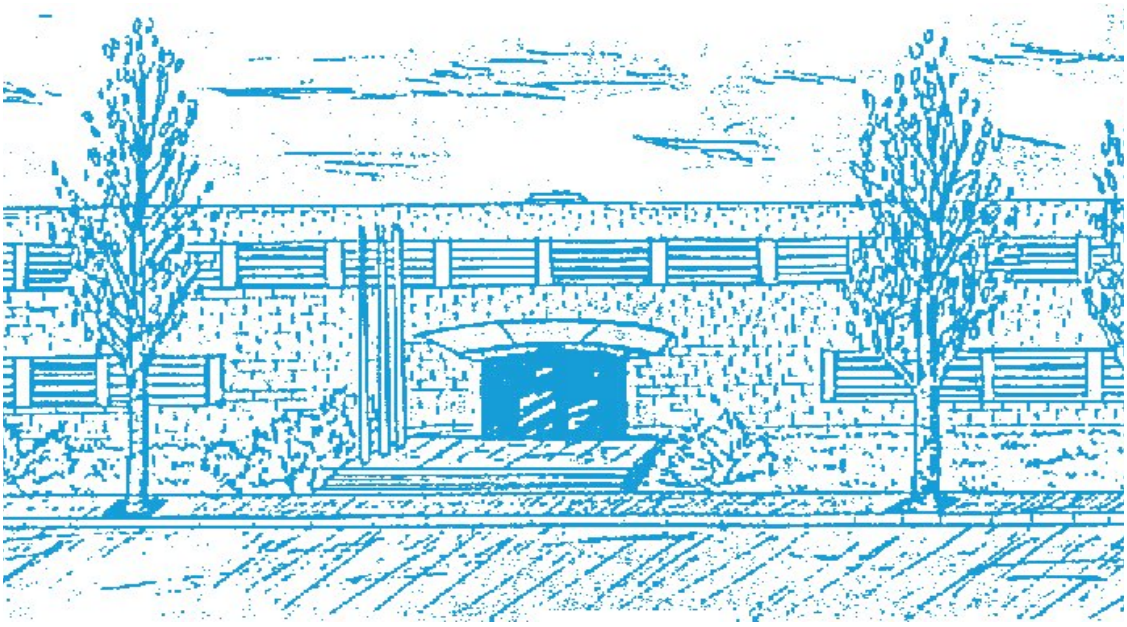

UNIVERSITAT POLITÈCNICA DE CATALUNYA
BARCELONATECH
Facultat de Matemàtiques i Estadística

Universitat Politècnica de Catalunya
Facultat de Matemàtiques i Estadística

Master in Advanced Mathematics and Mathematical Engineering

Master's thesis

Warmer temperatures and their effect on East-African malaria

Marta Pardo Araujo

Supervised by J. Tomás Lázaro Ochoa and David Alonso Giménez

June, 2020

I would like to thank some of the people who have helped me during this process and comment that even with the stress and the tension that I have suffered during these past months I have enjoyed a lot the work done and it motivates me to keep learning more and more about dynamical systems apply to epidemiology.
First, I would like to thank to J. Tomás Lázaro Ochoa who is an amazing professor and has helped me in the academic and in the emotional part, giving me the motivation and support to work hard, also he has helped me with the followings steps of my career, for what I am tremendous grateful. As well I would like to thank David Alonso Giménez who has helped me a lot presenting a more biological point of view of the problem.
Second I would like to thank my family who also have supported me and stayed close to me when I needed them, giving me the strength to reach every goal that I wanted to achieve. With an special word for Celsa, my twin, who is also a mathematician an always helps me with everything. To finish I would like to thank my friends who are always beside me, no matter what, with an special remark to Cris and Nico who have been sharing my stress and bad days to boost my confidence and happiness.

Thanks a lot to all.

Abstract

Malaria has been an issue worldwide for a long time, having a huge social, economic, and health burden. This disease occurs mostly in tropical and subtropical areas of the world, in countries where the levels of poverty are higher. In this work we will focus our study of malaria in Kenya. Because it has been an issue in this region for a long time. Due to insecticide and cool temperatures the disease was eradicated from Kenya's highlands in the 1960's. However, the disease has returned in recent years, as some researchers believe ([1],[3], [12]), that it is produced by subtle changes in the region's climate. We have strongly based our work in [1]. But, while they focus their study on the influence of climate change in the spread of malaria, we give a more qualitative approach of the model and present some feasible applications to other geographical regions. Moreover we introduce different rates to analyse the impact of a pandemic, like the basic reproduction rate $\mathcal{R}_0$.

Keywords

Malaria, Epidemiology, Dynamical systems, SIR models, Basic reproduction rate.

1. Introduction

Malaria has been an issue worldwide for a long time, having a huge social, economic, and health burden. Malaria occurs mostly in tropical and subtropical areas of the world, in countries where the levels of poverty are higher. In the majority of the countries were malaria is endemic, it is prime factor of illness and death. During 2018, it was estimated that 405.000 people died from the disease, the majority were young children in the sub-Saharian Africa. However, the Worlds Health Organization (WHO) says that the mortality of malaria has decrease around a 20% in the last decade, probably due to control measures and the development of clinical treatment against malaria.

Africa is one of the most affected continents due to the following factors: the high presence of the mosquito vector responsible of the disease transmission to humans, the predominance of the parasite species *Plasmodium falciparum*, which is the specie responsible of severe malaria and death, the local weather conditions and the scarce resources combined with a socio-economic instability which decreases the effectiveness of control effort.

Due to the high mortality and the presence of the disease all around the world Malaria have been studied by numerous epidemiologists for the last decades. First Charles Louis Alphonse Laveran, a French army doctor, observed the parasite inside the red blood cells of an infected people and after that Sir Ronald Ross proved the complete life-cycle of the malaria parasite in the mosquitoes. Although the disease has been study for many years it is still a major public health problem. Because there is no effective vaccine and, since the parasite evolved drug resistance, many of the anti-malarial drugs are losing effectiveness.

In the past 100 years mathematical models have been used to provide an explicit framework for understanding malaria transmission dynamics in human population. This work started with Ronald Ross ([4]), who presented a simple model to prove that malaria could be eradicated simply by reducing the number of mosquitoes. And subsequently George Macdonald in [16] presented a highly improved model, focused on the mosquito eradication.

In this work we will focus our study of malaria in Kenya. Malaria has been an issue in Kenya for a long time. Due to insecticide and cool temperatures the disease was eradicated from Kenya's highlands in the 1960's. However, the disease has returned in recent years, as some researchers believe ([1],[3], [12]) that it is produced by subtle changes in the region's climate. We have strongly based our work in [1]. But, while they focus their study on the influence of climate change in the spread of malaria, we give a more qualitative approach of the model and present some feasible applications to other geographical regions.

In the first section we give an explanation of the model and a detail description of the important parameters, giving a clear view of the importance of temperatures and rainfall in the model. We also prove that the solutions of the ODE governing the carrying capacity of the mosquito tend to a periodic solution, due to the (approximate) periodicity of the rainfall. Along the second section we show the results of the numerical simulations obtained by integrating the model with a Runge-Kutta method. For that we use the climate data given in [1]. In addition we expose some interesting insights that we have observed from the results of the integration. We also explain the numerical tools used for the simulations and the difficulties that has been presented along the process.

In the third section we introduce the basic reproduction rate $\mathcal{R}_0$, and the algorithm developed by Diekmann and Heesterbeek [8] to compute it. In addition we present an interesting example to give a better understanding of the algorithm. We have applied the algorithm to compute the basic reproduction rate for COVID-19, in [14] (they compute $\mathcal{R}_0$ for a simple model of COVID-19). Since we did not agree with this computation we modified it and presented as an example of the Diekmann and Heesterbeek algorithm. Moreover we give an sketch explanation of the method used in [1] to compute $\mathcal{R}_0$. During the third section we show in detail our computation of the basic reproduction rate for the human-mosquito model. We present commonly used parameters which estimate the mortality risk of a disease, like the case mortality rate or the crude mortality rate.
In the last section we apply the model to different location, a village located in the Spanish Mediterranean coast, Agost, to introduce an interesting further study: the probability of a pandemic outbreak in Mediterranean region. To conclude we explain the knowledge acquired during this master's thesis.

2. Explanation of the Model

2.1 Human component

In this work, we study a malaria population model presented in [1] which couples the dynamics of the disease in the mosquito vector and the human host. These two components are modeled with a variation of a SIR model ([21], [6]). The SIR models are used to model epidemics. The particularity of this type of models is that they divide the host population into three different classes: infected, susceptible and recovered, which are called compartments.

We present a variation of the SIR with higher complexity. Since both of then, the human and the mosquito are host for the infection, they are divided on its turn in different compartments depending on the infection state of the individuals.
To complete the model, the human and the mosquito equations are coupled through two variables: one which determines the human infections produced by the infectious mosquitoes Λ and y which is the fraction of infected humans that a mosquito can bite and therefore get infected and become infectious. These two ways of coupling the system is due to the fact that the human gets infected by the mosquito and vice versa. Later on we will give a more detailed explanation of these two variables.
In our model the human population is split into different classes, in fig. 1 there is a diagram of the human-mosquito model to give a clear view of the flow between the different compartments.

For the human component there are two types of infected individuals (E), the ones which develop symptoms, given by a probability ξ and therefore receive some treatment (C); and the individuals which are infected but have not present symptoms. Even though, they can transmit the parasite to the vector (I).
Another group is formed by the individuals who are recovered from the disease (R), whether they have cleared parasitaemia or have too low levels of it to infect the vector. Another type of individuals is the one which are susceptible to be infected (S), which is composed by the births and migrations (B), and the individuals who have recovered and loses immunity at rate σ. The sum of the total population N is assumed to be constant constant and so births and migrations balance with the loss due to mortality, given by the population turnover δ_H, which is also taken as constant.

The system of differential equation which describes the dynamics of the human population is given by:

$$\begin{aligned}
\frac{dS}{dt} &= B - \beta S + \sigma R - \delta_H S + \rho C \\
\frac{dE}{dt} &= \beta S - \delta_H E - \gamma E \\
\frac{dI}{dt} &= (1-\xi)\gamma E - \eta\beta I + \nu C - rI - \psi I - \delta_H I \\
\frac{dR}{dt} &= -\sigma R + rI - \delta_H R \\
\frac{dC}{dt} &= \xi\gamma E + \eta\beta I - \nu C - \rho C - \alpha C - \delta_H C
\end{aligned} \tag{1}$$

The recovery of individuals depends on the group of the population, for individuals belonging to the asymptomatic infected class (I), they recover at rate r while for individuals in class C they recover at rate ρ and become part of the susceptible class (S). The loss of population is due to migrations and mortality. The mortality which is related to the malaria is measured through ψ and α for classes I and C respectively. The susceptible individuals S are in the exposed phase, the period when they can get the malaria, in average this time span is given by $1/\gamma$.

One of the most complex process is the host's immune response. In [1] they consider two main factors,

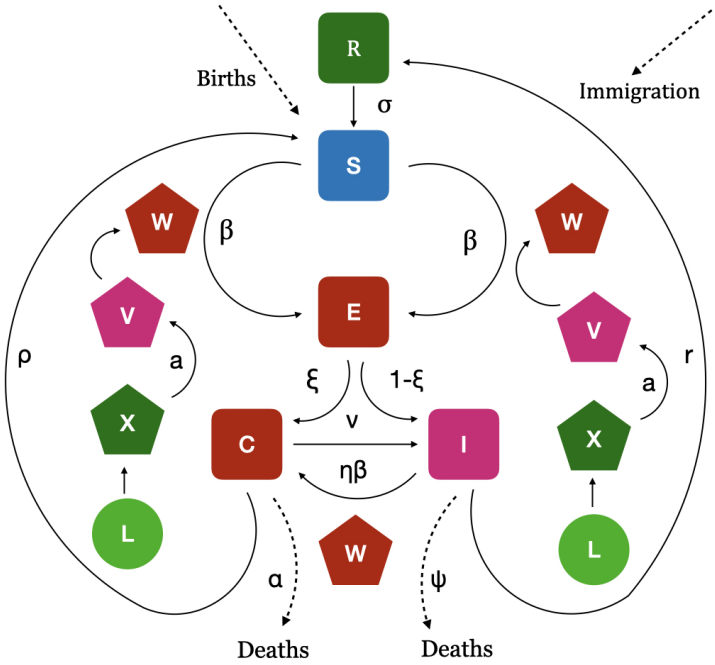

Figure 1: Diagram of the human-mosquito model.

the *rate of loss of immunity* σ and the *recovery rate* r. Which are given by:

$$\sigma(\Lambda) = \frac{\Lambda}{\exp(\Lambda/\sigma_0) - 1} \tag{2}$$

$$r(\Lambda) = \frac{\Lambda}{\exp(\Lambda/r_0) - 1} \tag{3}$$

where $\Lambda = aW/N$, W is the total number of infectious mosquitoes and $N = S + E + I + R + C$ is the total human population. We denote as σ_0 and r_0 the respective basal rates when Λ tends to zero,i.e the total number of infectious mosquitoes tends to zero (there is no disease transmission).
As figures 2 and 3 show the recovery rate and the loss of immunity versus the total number of infectious mosquitoes, respectively. Note that both functions are decreasing functions with respect to the number of infectious bites per human. When Λ the mosquito pressure in human is high the disease clearance becomes smaller. If Λ is measured in years it is called the entomological inoculation rate (EIR), which is a measured of exposure of infectious mosquitoes.

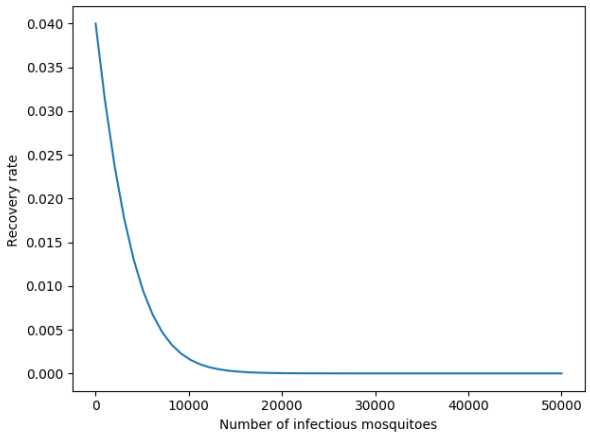

Figure 2: Recovery rate, r, for a biting rate $a = 0.952$ and $r_0 = 0.04$.

The total population N is assumed to be constant, since the replenishment of new susceptible individuals through immigration or births (B) is balanced with the loss of individuals due to mortality. As we can see in the equations:

$$\dot{N} = \dot{S} + \dot{E} + \dot{I} + \dot{R} + \dot{C} = B - \delta N - \psi I - \alpha C$$

In [1] it is assumed that $B = \delta_H N$ and $\psi = \alpha = 0$ then $\dot{N} = 0$. Therefore the population remains

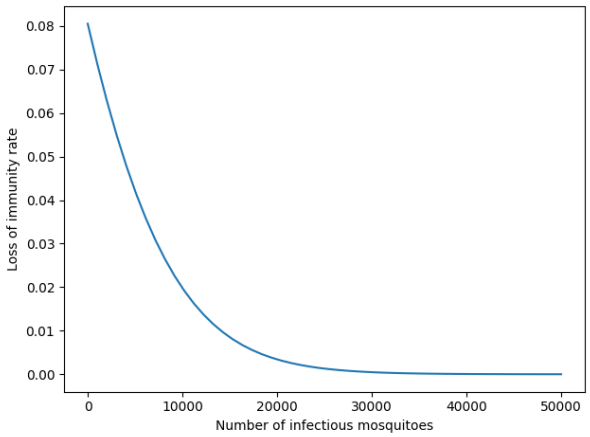

Figure 3: Loss of immunity, σ, for a biting rate $a = 0.952$ and $\sigma_0 = 0.0805$.

constant. Thus the system (1) becomes:

$$\begin{aligned}
\frac{dS}{dt} &= \delta_H(E + I + C + R) - \beta S + \sigma R + \rho C \\
\frac{dE}{dt} &= \beta S - \delta E - \gamma E \\
\frac{dI}{dt} &= (1 - \xi)\gamma E - \eta\beta I + \nu C - rI - \delta_H I \\
\frac{dR}{dt} &= -\sigma R + rI - \delta_H R \\
\frac{dC}{dt} &= \xi\gamma E + \eta\beta I - \nu C - \rho C - \delta_H C
\end{aligned} \tag{4}$$

The system (4) given bellow is a non linear system of ODE's. Due to β the force of infection or transmission rate, the recovery rate, r, and the loss of immunity rate, σ the dynamics between the human and mosquito component are coupled.

The Force of infection β: The *force of infection* β is the per capita probability at which susceptible individuals get infected through bites of infectious mosquitoes. This rate depends on the immune response of the individual to the disease, higher is the immune response lower is the probability of developing malaria, this is measured by b. Also, it depends on the frequency of mosquito bites per human a and in the number of infectious mosquitoes W. Therefore the local force of infection is as follows:

$$\beta = b\frac{W}{N}a, \tag{5}$$

where remind that N is the total number of human population. Since the process of the parasite to make a mosquito infectious, after it have got the disease, takes some time, the mosquitoes which are infectious at time t come from a mosquito which have bitten infected humans previously.
There are external force of infection measured by β_e. This force measures the imported malaria cases, which are related to the individuals who get the disease when travelling to an endemic country. The expression for β given in (5) describes the local force of infection, which is produced by infectious mosquitoes in the

region. Thus the force of infection will be measured as a sum of these two components, the local force of infection and the external one. Then we have that:

$$\beta = b\frac{W}{N}a + \beta_e. \tag{6}$$

Note that this external force is assumed constant, in order to simplify the model.

2.2 Mosquito component

Now we present the mosquito component. It is divided in two main categories: the larvae (L) and the adult mosquitoes (M). The population of larvae L varies as follows:

$$\frac{dL}{dt} = fM\left(\frac{K-L}{K}\right) - \delta_L L - d_L L \tag{7}$$

where K is the carrying capacity, which is the maximum number of larvae that the ecosystem can sustain, f is a per-capita fecundity rate, d_L is the development rate and δ_L the mortality rate. It has been studied that mosquito females lay eggs only between meals, so the fecundity rate is related to the biting rate as follows: $f = Fa$.
The adult mosquito population M is composed by three different types of individuals, the non-infected mosquitoes (X), infected and non- infectious (V) and the infectious mosquitoes (W), then $M = X+V+W$. We denote by y as the fraction of infectious human, then $y = (C+I)/N$.
The variation of each class is modelled as follows:

$$\begin{aligned}
\frac{dX}{dt} &= -cayX - \delta_M X + d_L L \\
\frac{dV}{dt} &= cayX - \gamma_P V - \delta_M V \\
\frac{dW}{dt} &= \gamma_P V - \delta_M W
\end{aligned} \tag{8}$$

where d_L is the mortality rate of adult mosquitoes and γ_P is the per capita rate at which new infectious mosquitoes arises. This is related to the time of sporogony.

Some of the parameters of the model depend on temperature and rainfall, which are a key factor in the development of mosquito from larvae to adult mosquito. Indeed in [1] it has been shown an influence between the rise in temperature due to climate change and the propagation of malaria. In this work we will do a qualitative analysis rather than a quantitative analysis as it has been done in [1].
The temperature and rainfall data is taken daily and monthly respectively. We use a cubic spline method in order to interpolate the time function for rainfall and temperature. This method is explained in detail in appendix A.
The following parameters are functions which depend on empirical data:

1. **Development rate of the mosquito vector,** d_L**,** is the amount of time spend in the larvae stage is given by a regression:

$$d_L = \begin{cases} 0.00554T - 0.06737 & \text{if } T > 12.16^\circ \\ 0 & \text{otherwise} \end{cases} \tag{9}$$

   where T is the temperature in Celsius degrees.

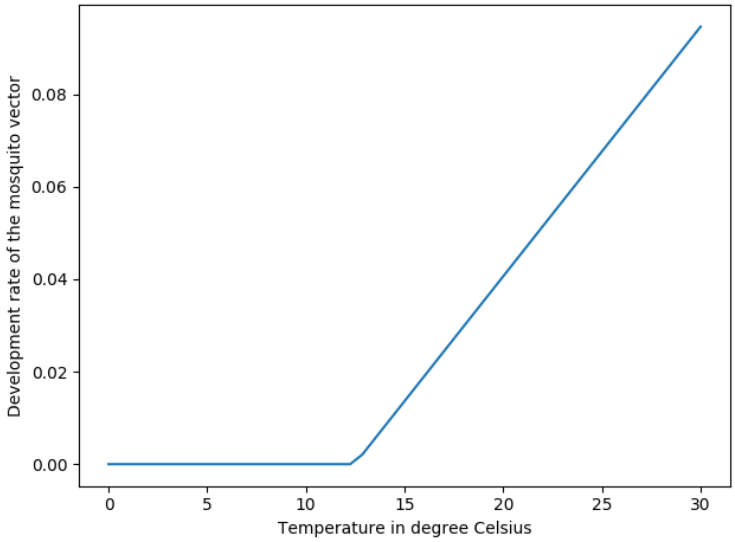

Figure 4: Development rate of the mosquito vector, d_L

2. **Development rate of the Plasmodium parasite,** γ_P**,** is the period of time from when the mosquito bites a human with malaria until it becomes infectious, i.e when it can transmit the parasite to humans by the saliva. It is given by a regression:

$$\gamma_P = \begin{cases} 0.009T - 0.1441 & \text{if } T > 16.01^\circ \\ 0 & \text{otherwise} \end{cases} \tag{10}$$

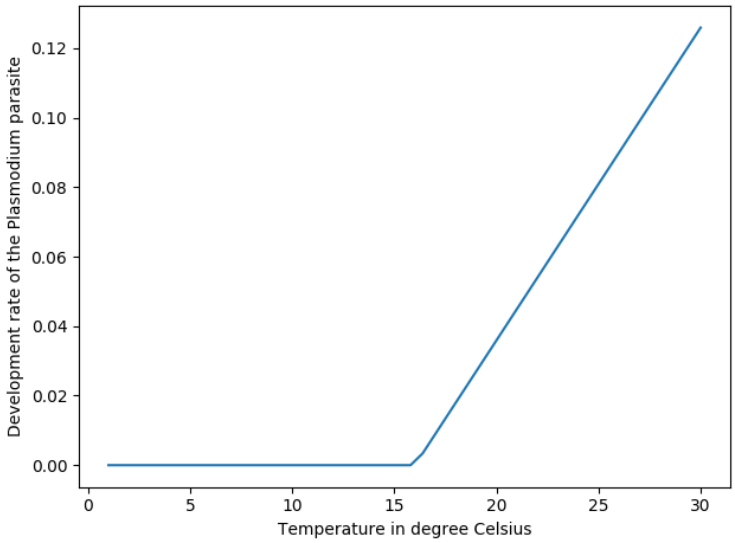

Figure 5: Development rate of the *Plasmodium* parasite, γ_P

3. **Death rate of adult mosquitoes, δ_M:**
   The death rate of adult mosquitoes is given by :

$$\delta_M = \frac{1}{\lambda}, \tag{11}$$

   where λ the average life time of adult mosquito which depends on temperature as follows:

$$\lambda = -4.4 + 1.31T - 0.03T^2. \tag{12}$$

   Figure 6 shows the average life time for adult mosquito, when $T \approx 21.83$ (approximately 10 days) there is a maximum.
   In equation (11) there is a critical point for values of λ close to 4 and 40 degrees Celsius, which is shown in fig. 7.

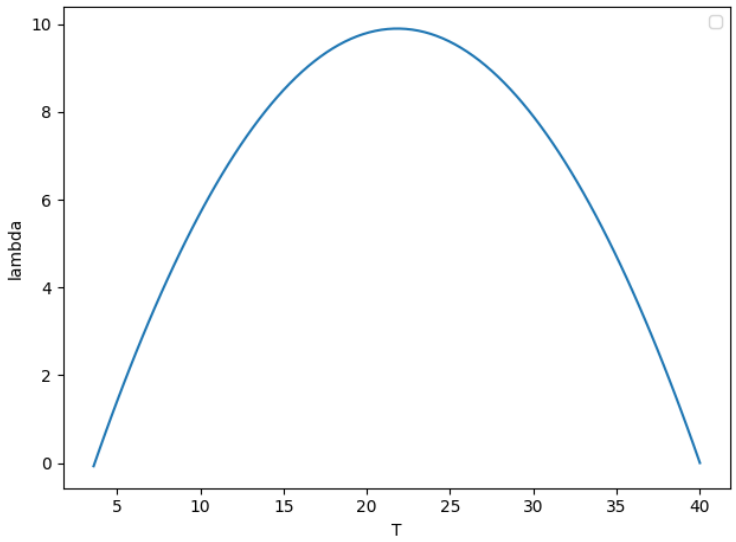

Figure 6: Average life time for adult mosquitoes depending on temperature measure in Celsius degrees

4. **Death rate of mosquito larvae, δ_L,** in order to express the daily larval survival we take a slightly different approach from [1]. We modify the component of the mortality rate of larvae depending on temperature.
   The effect of temperature and rainfall in larvae mortality has been studied in [5], where is given data of larval average life time (the inverse of the per capita death rate, δ_L) for a given temperature (from 10 to 40 Celsius degrees). We approximate the missing values, $\delta_L(T)$, as follows:

$$\delta_L(T) = \frac{\delta_L(T_k) + \delta_L(T_{k+1})}{2}, T \in (T_k, T_{k+1}) \tag{13}$$

   where $\delta_L(T_k)$ and $\delta_L(T_{k+1})$ are given in [5]. To obtain this values the study was conducted in the laboratory. The authors do not take into account the mortality due to predators or any other source.

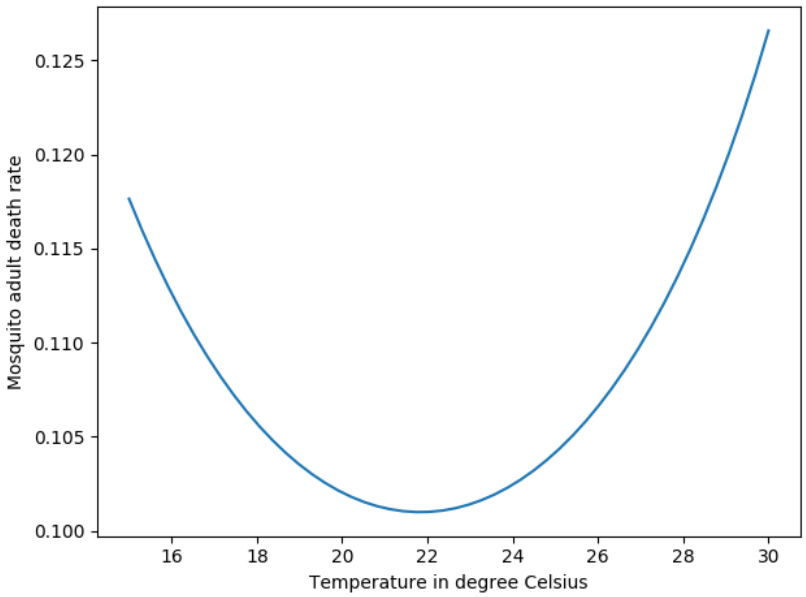

Figure 7: Plot of the mosquito adult death rate, δ_M, depending on temperature measure in Celsius degrees, we have represented the interval of 15 to 30 degrees.

They state that 20% of the larvae will fail to develop into adult mosquitoes. Therefore in [1] the mortality death rate of larvae is given as follows:

$$\delta_L = \delta_0 + \delta_L(T) + \tilde{\delta_L}(P), \tag{14}$$

where δ_0 is the basic mortality rate which is independent of temperature and rainfall.
Another cause of mortality is the rain peaks which are measured by :

$$\tilde{\delta_L}(P) = \delta_R \Theta(P - \langle P \rangle_{12}), \tag{15}$$

where $\langle P \rangle_{12}$ is the moving average computed from the rainfall data and

$$\Theta(x) = \begin{cases} x & \text{if } x > 0 \\ 0 & \text{otherwise} \end{cases} \tag{16}$$

where δ_R is a proportional factor transforming a positive deviation from the moving average, due to a peak in rainfall, into a increase in larval mortality.

5. **Gonotrophic cycle, mosquito fecundity and biting rate,** the gonotrophic cycle or the reproductive cycle of the mosquito includes the searching for a host, blood feeding, blood meal digestion, egg maturation and oviposition. Oviposition last approximately between two and eight days depending on the temperatures. We use the data presented in [2] since we wanted to take a different approach than in [1]. In this work it has been studied the influence of temperatures in the gonotrophic cycle in the Western Kenya Highlands.
Hematophagous mosquitoes need blood meals for egg development and the rate of blood meal digestion is temperature-dependent. The higher the temperatures the faster is the digestion, as a consequence, the shorter will be the gonotrophic cycle duration. This will imply that the biting rate

is higher. The inverse of the average gonotrophic cycle, denoted by $\langle t_a \rangle$, is approximately the biting rate (a). To approximate the mean gonotrophic cycle duration we compose a piecewise function. This function will depend on the season of the year. Thus the $\langle t_a \rangle$ is as follows:

$$\langle t_a \rangle = \begin{cases} 2.9 & \text{if t is in the dry season} \\ 8.6 & \text{otherwise} \end{cases} \tag{17}$$

In the case of Kenya the rainy season will be from February to May and from September to November.

At the end of the gonotrophic cycle, females lay a number of eggs. This is given as follows:

$$N_f = na \tag{18}$$

where n is the number of eggs at each oviposition, then the maximum number of eggs that enter the larval stage per female per unit time is $f = Fa$.

2.3 Larval Carrying Capacity

The Larval Carrying capacity is the maximum amount of larvae in a given ecosystem, in [1] it is model with a differential equation depending on rainfall, P, as follows:

$$\frac{dK(t)}{dt} = K_A P - K_E K(t). \tag{19}$$

Where $K_A P$ determines the increase in the carrying capacity due to daily precipitation.
The equation (19) admits a unique periodic solution, of period T, which is denoted by $K_p(t)$. This is the solution of the Cauchy problem associated:

$$\begin{cases} K'(t) = K_A P - K_E K(t) \\ K(t_0) = K_0. \end{cases} \tag{20}$$

In our problem we can assume that $t_0 = 0$, so we have that $K(0) = K_0$.
We know, from the theory of differential equations, that the solution of a linear non homogeneous ODE of the form $x' = ax + f(t)$, is given by :

$$x(t) = x_h(t) + x_p(t) = ce^{at} + \int_{t_0}^{t} f(s)e^{a(t-s)}ds \tag{21}$$

where x_h is the solution of the homogeneous equation and x_p is the particular solution. So for the Cauchy problem (20) we have the following solution:

$$K(t) = K_h(t) + K_p(t) = k_0 e^{-K_E t} + \int_{t_0}^{t} f(s)e^{-K_E(t-s)}ds \tag{22}$$

and $\forall k_0 \in \mathbb{R}$ and every solution $K(t)$ we have that :

$$\lim_{t\to\infty} |K(t) - K_p(t)| = \lim_{t\to\infty} k_0 e^{-K_E t} = 0 \tag{23}$$

since $K_E > 0$. This means that after some time every solution will tend to the periodic solution, $K_p(t)$ which corresponds to the period of rains, which it will be approximately one year and we will show later on in the obtained simulations.

2.4 Full Model formulation

The whole system of equations for the human-mosquito is given by:

$$\begin{aligned}
\frac{dS}{dt} &= \delta_H N - \beta S + \sigma R - \delta_H S + \rho C \\
\frac{dE}{dt} &= \beta S - \delta_H E - \gamma n_H E \\
\frac{dI}{dt} &= (1-\xi)\gamma n_H E - \eta\beta I + \nu C - rI - \delta_H I \\
\frac{dR}{dt} &= -\sigma R + rI - \delta_H R \\
\frac{dC}{dt} &= \xi\gamma n_H E + \eta\beta I - \nu C - \rho C - \delta_H C \\
\frac{dL}{dt} &= faM\left(\frac{K-L}{K}\right) - \delta_L L - d_L L \\
\frac{dX}{dt} &= -cayX - \delta_M X + d_L L \\
\frac{dV}{dt} &= cayX - \gamma_P n_P V - \delta_M V \\
\frac{dW}{dt} &= \gamma_P n_P V - \delta_M W \\
\frac{dK}{dt} &= k_A P - k_E K
\end{aligned} \tag{24}$$

3. Kericho data simulations

Malaria has been an issue in Kenya for a long time. Due to insecticide and cool temperatures the disease has been eradicated from Kenya's highlands in the 1960's. However the disease has returned in recent years, as some researchers believe ([1],[3], [12]) that it is produced by subtle changes in the climate region. In this section we present the numerical results that we have obtained using the data of Kericho, a village in a tea plantation, which is located in the Kenya's highlands. Also we give some insights about the results and about the problems that we have encounter during the process.

We have implemented a program in C using a rk78 integrator, to numerically integrate the equations presented in (24), to observed the solutions and study how the disease propagates along time.
The rk78 is an Adaptive Runge-Kutta-Fehlberg method. We have chosen it due to the following advantages: smaller errors and adaptative time step (h). Since it uses two rk methods one of order 7th and the other of order 8th. Assuming that the last one is very close to the exact solution since it is more accurate. It will modify the time step according to the distance between the solutions of the two numerical methods. Some difficulties were presented along the process. First of all the climate data given in [1] is a discrete set and we need a continuous set as a input of the model. Since the data taken from [1] for the temperature and rainfall is given monthly and daily respectively, we have implemented a method to interpolate the data. For this task we have chosen the cubic splines which gives an interpolating polynomial.
This method satisfies some convenient properties: it avoids the Runge's phenomenon and second, it is also

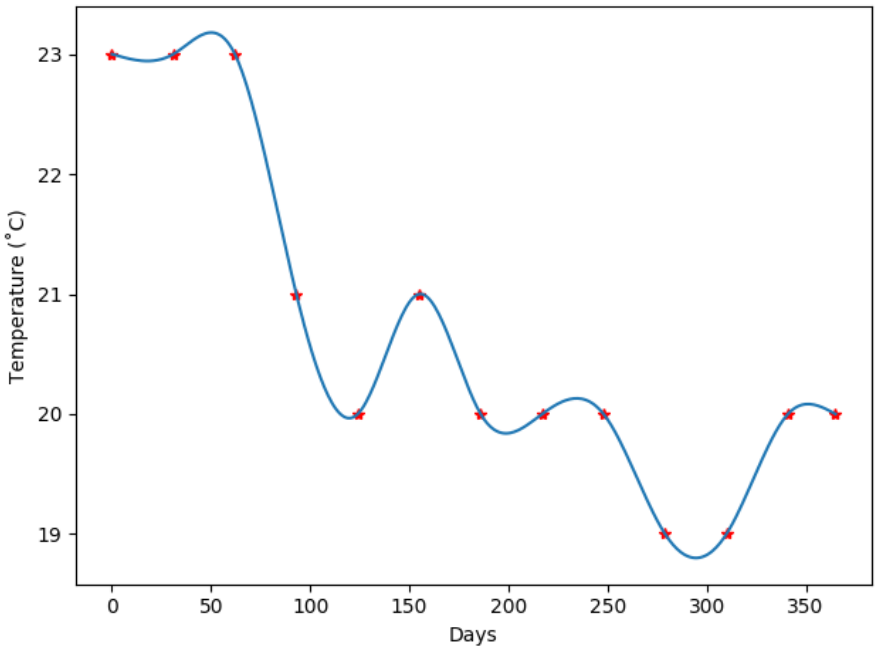

Figure 8: Average temperatures from 1st December to 1st November of 2003 in Kericho, Kenya. Measured in degrees Celsius.

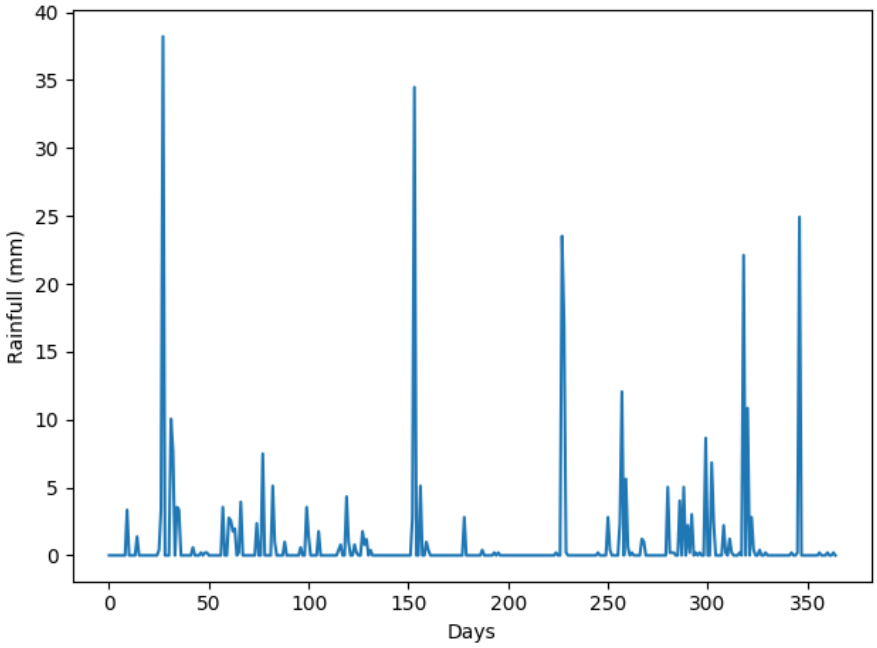

Figure 9: Rainfall from 1st December to 1st November of 2003 in Kericho, Kenya. Measured in mm.

easily computable. More detailed explanation of the method is given in the appendix A.
Another issue presented during the implementation was the memory usage, since we will need to store many different variables along the integration and also the interpolation. We have implemented a memory structure based on pointers to optimise the memory usage.
For our simulations we have used the climate data in [1] from January of 2002 to December of 2002. This data is monthly for temperatures and daily for rainfall.
Figure 9 shows the rainfall in mm during this period, as we can observed the rainy seasons goes from February to May and from August to November, i.e where the amount of rain is higher. In fig. 8 we can observe a plot of the average temperature: the red starts denotes the data taken from [1] while the blue lines denotes the interpolation done with the splines. As we can see the splines are $\mathcal{C}^2$ smooth and fit the same value as the real data in the endpoints of the intervals (the start and the end of each month).
In the other hand we have used the values of the parameters given in table S1 in [1], the authors have used a genetic algorithm for this propose. We have not get into the fitting parameter problem since this belongs to the optimization field and is out of the scope of this work.
After we got the data from the C program we use Python to plot the output of the algorithm and some other interesting graphs which can give an intuitive overview of the problem.

For our simulations we have used the following initial conditions: constant human population set to

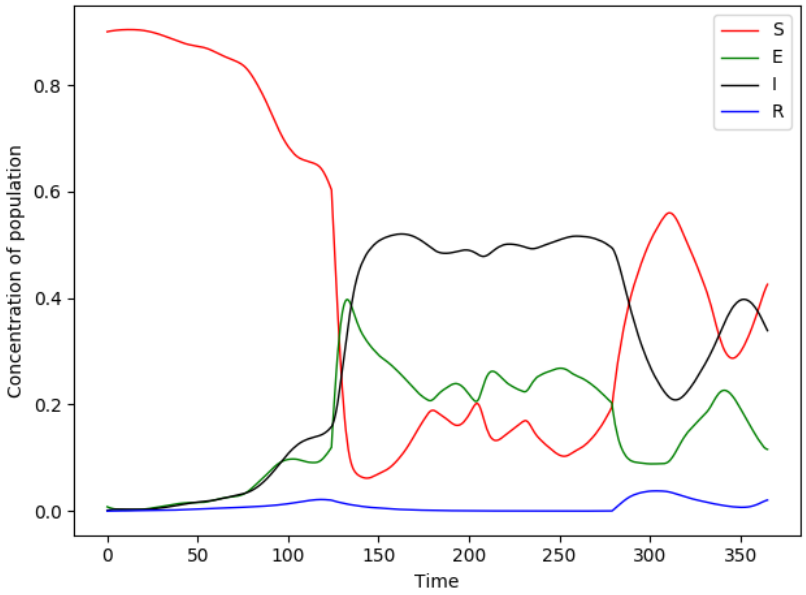

Figure 10: Numerical simulations of the model for the SEIR population normalized by the total population.

50000, where the 90 % of the population is susceptible and there are no recovered people. The values of the parameters are presented in table 1.

Figure 11 shows the susceptible (S), exposed (E), asymptomatic infected (I) and recovered (R) individuals over time. As we can observe the susceptible individuals start to decrease from the beginning of the simulations, these individuals go to the exposed individuals by a factor β, which is the force of infection. After a short period of time there is an increase of I, which are the asymptomatic infected individuals.

Model Parameter	Symbol	Range	CI
Human turn-over rate	δ_H		$1/20$ year^{-1}
Mosquito fecundity factor	F		66
Loss of immunity rate	σ_0	(0,0.1)	0.0805
Recovery rate	r_0	(0,0.1)	0.04
Exposed number	n_H	(1,50)	3.07
External force of infection	β_e	$(0, 10^{-4})$	2.57e-05
Detection probability ($S \to C$)	χ	$(0, 0.5)$	0.131
Recovery rate ($C \to S$)	ρ	(0,1)	0.428
Case Probability ($I \to C$)	η	(0,0.1)	0.0346
Recovery rate ($C \to I$)	ν	(0.2,1)	0.564
Probability ($M \to H$)	b	(0.5,1)	0.649
Probability ($H \to M$)	c	(0.1,1)	0.365
Death rate larvae	δ_P	$(0.01, 0.5)$	0.0329
Death factor larvae	δ_R	$(0, 0.5)$	0.00783
Conversion factor	K_A	$(0, 3 \cdot 10^3)$	695
Loss rate	K_E	(0,0.3)	0.198
Exposed number	n_P	(1,50)	8.99
S initial fraction	y_S	(0.9,1)	0.99
E initial fraction	y_E	(0,0.02)	0.008
I initial fraction	y_I	(0,0.02)	0.0011
C initial fraction	y_C	(0,0.01)	0.0009

Table 1: In this table it is shown the list of parameters. The two first parameters are left constant, while the others can vary between a range. In our simulations we have used the average value in the range of the parameters.

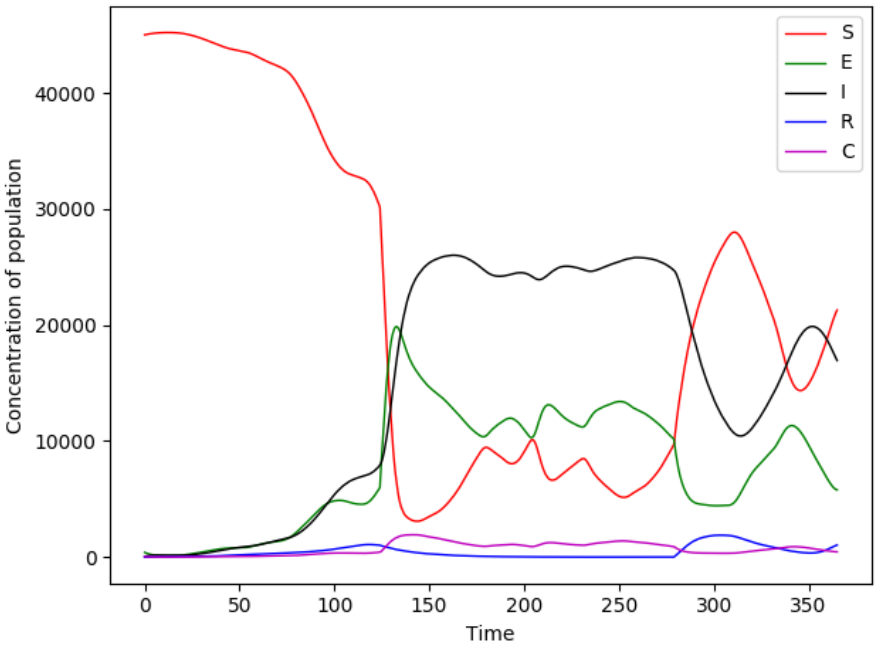

Figure 11: Numerical simulations of the human model over the 2002 year.

First, we will study the human population and after that the mosquito component to give a clear view of the results. In fig. 13 a plot of the total human population including the C population, which are the individuals who got clinical treatment, is presented. We can observed that the C individuals experiment an increase from May to September as it does for the asymptomatic individuals, I. After some fluctuations around the 300 day the susceptible individuals start a sharp increase while the infected individuals, I and C, decrease.

Figure 12 shows the data taken from [1] of the accumulated hospitalized individuals in Kericho. As we can see there is a maximum around May and a relative minimum around September as it happens in the simulations for the clinical cases, C, presented in fig. 13.

Now we give some insights about the mosquito component, splitting the population between the larvae and its carrying capacity, and the adult mosquito. In fig. 14 and fig. 15 there are plots of the simulations over a year for the mosquito component. In the first one the whole mosquito population and the carrying capacity related to them is represented .In the second one there is a plot of the adult mosquito population to give a more clear view of the solutions. As we can observed the total number of larvae goes to the maximum size possible restricted by the carrying capacity at the beginning of the simulations, and it keeps with this behaviour until the end of the year. The carrying capacity is directly related to the amount of rain, as we have explained in section 2.3, after some time the solutions tends to the periodic solution which its period is approximately one year. Figure 17 shows the simulations produces by the model along three years, we can observe that the solutions tends to a periodic solution with period one year.

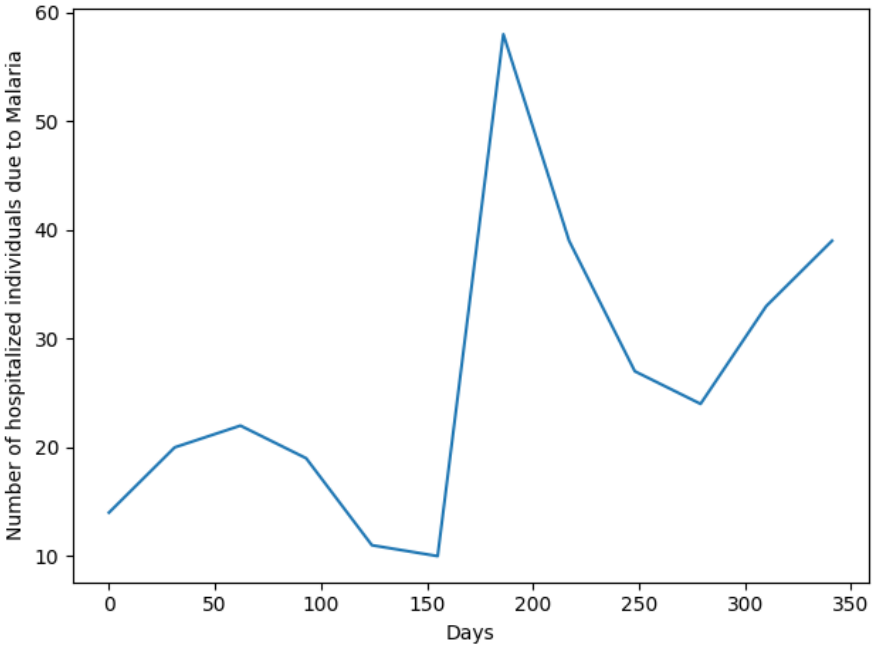

Figure 12: Number of individuals hospitalized cases of malaria in Kericho in 2002.

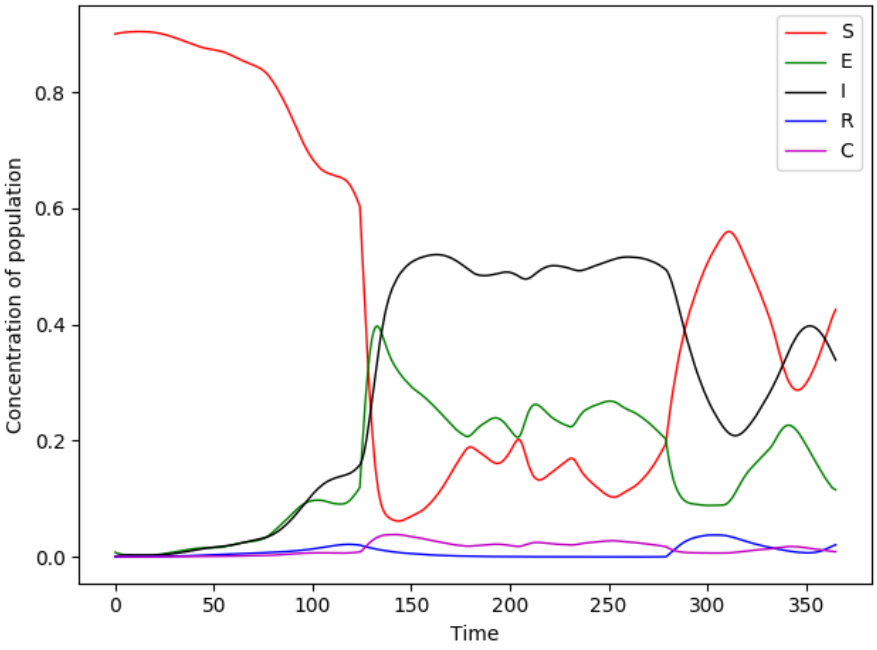

Figure 13: Numerical simulations of the model for the human population normalized by the total population.

In the other hand, since X increases by a factor d_L times the amount of larvae the uninfected adult mosquito population, X, increases at the beginning with some delay respect to the larvae. This is due to the fact that it is an increasing function for temperatures greater than approximately 13°, as we can see in fig. 4.

The decrease on the X population, around the 150 day, is due to the transition of this individuals to the compartments of the infected mosquitoes, the non infectious and the infectious one, V and W respectively. This agrees with the increase of the temperatures from 20 to 21 degrees. In the other hand the increase on the infectious mosquitoes is faster than in the non infectious due to the increase of the development rate of the Plasmodium parasite, γ_P since the temperatures are over 20 degrees in this period. We can observe in fig. 5 that the development rate of the Plasmodium overcomes values of 0.03 for temperatures greater than 20 degrees.

If we compare the two components, the human and the mosquito, we can give a general view of the

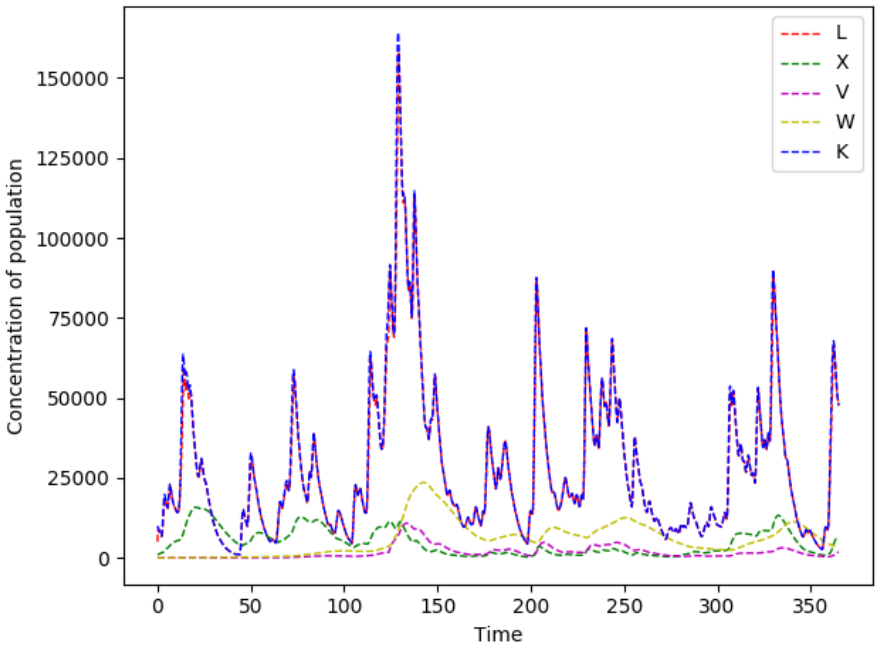

Figure 14: Numerical simulations of the model for the mosquito population and the carrying capacity related to them.

problem. Notice that there is a relation between the increase of the infectious mosquitoes and the increase of the infected individuals and viceversa around the 5th month, May. This is due to the force of infection β which is directly proportional to the total number of infectious mosquitoes and the fraction of infected individuals y which produces an increase in V, the infected mosquitoes. Also there is a decrease on both infected population when the temperatures decreases under 20 degrees.

First we have studied the behaviour of the solutions for one year and now we analyze the solutions for a longer period, three years. For these simulations we have use the same climate data from 2002 to 2004.

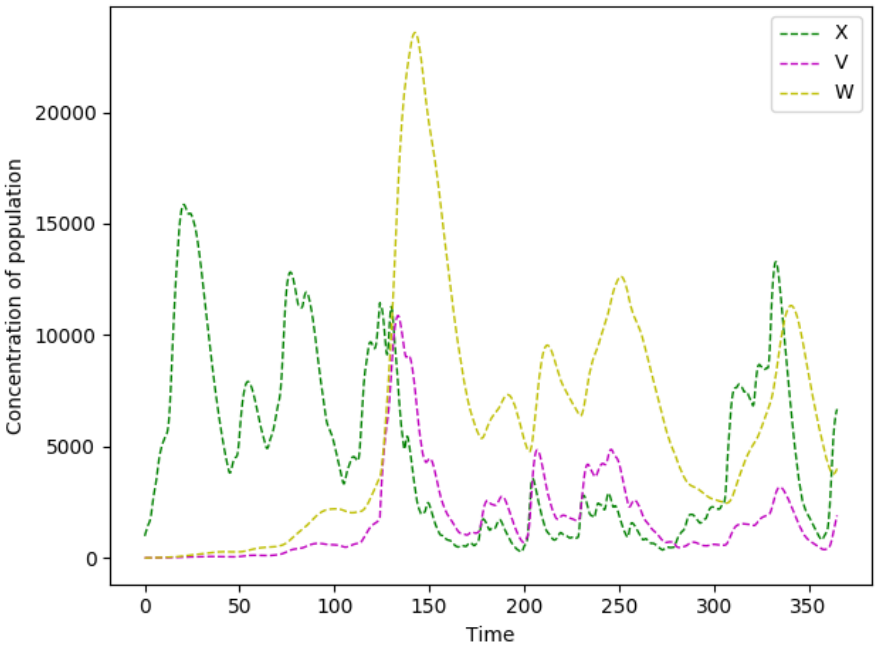

Figure 15: Numerical simulations of the model for the adult mosquito population.

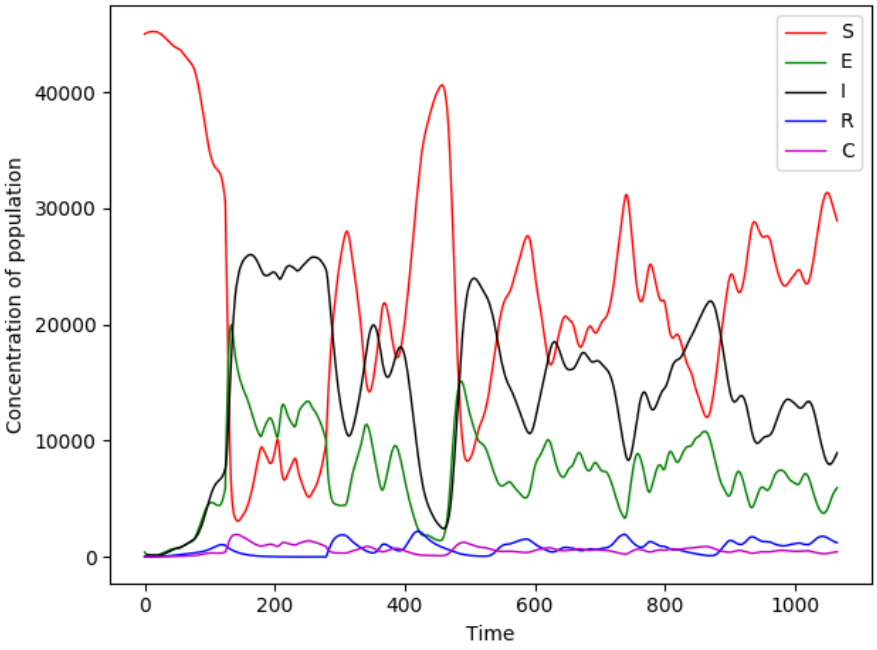

Figure 16: Numerical simulations of the model for the human population over three years, from 2002 to 2004.

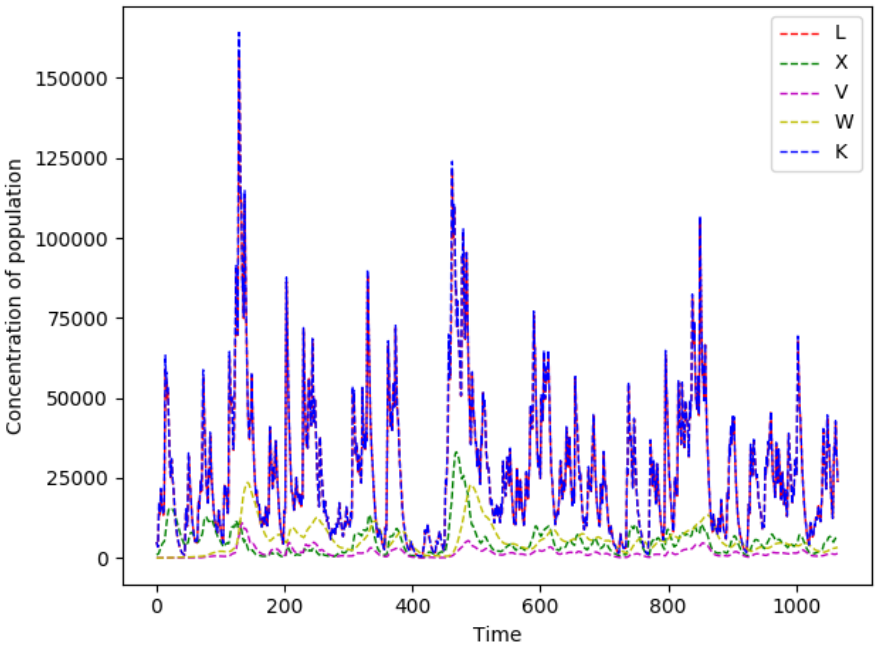

Figure 17: Numerical simulations of the model for the mosquito component over three years, from 2002 to 2004.

Figures 16 and 17 show the simulations for the human and mosquito component respectively. Notice that there is an important decrease on the infected individuals in the middle of the second year (around the 500 day) for the human component, corresponding to a decrease in the total adult mosquito population as we can observe in fig. 17. In addition, the total number of infected individuals shows a decreasing trend over the years, while the susceptible individuals are predominant among the population, in general, over the second and third year.

4. The basic reproduction rate $\mathcal{R}_0$

4.1 What is $\mathcal{R}_0$?

The term *"basic reproduction rate"* was first introduced to epidemiology by Macdonald in [15] in 1952 in the context of malaria. He explained $\mathcal{R}_0$, *"The number of infections distributed in a community as the direct result of the presence in it of a single primary non-immune case."* After him Smith C. in [20] applied this rate in his work about the arboviruses.
The concept of basic reproduction rate assumes that one infected individual enters a large population of susceptible individuals, during the period of infectiousness. Therefore, the initial spread of the disease can be approximated by a branched process, which is related to "traceability", where the spread of the disease is represented as a tree. This does not take into account the decrease in the susceptible population in next generations. Therefore the computation of the basic reproduction rate is a key factor to understand the

evolution of the disease in its firsts states. From the threshold $\mathcal{R}_0$ we have the following statement: If $\mathcal{R}_0 \geq 1$ then there will be a epidemic whereas if $\mathcal{R}_0 < 1$ one expect the disease under control. This $\mathcal{R}_0$ is related to the Malthus parameter r as we will proof later on. In [11] more detailed information about this rate is given, as well as different process to estimate it.

One of the most famous algorithm to compute the basic reproduction rate is the one done by Diekmann et al. in [8]. In this work a method to compute $\mathcal{R}_0$ through the so called Next Generation Matrix in compartmental epidemic models is shown.

4.2 O. Diekmann and J. A. P. Heesterbeek Algorithm

This algorithm is used for models which divide the population by traits (age, size or state of infection) into a finite number of categories (compartments). One can define the newly infected individuals in each compartment in following generations through the coefficients of the so called Next Generation Matrix (NGM) which is usually denoted by K. This matrix was introduced by Diekmann *et al* in [9]. They also introduced the term *infection free state*, which is the equilibrium point where the compartments corresponding to infected individuals are zero.
First we need to divide the system of equations in two subsystems: the one corresponding to the infection states and the rest. The first subsystem is also divided into two categories: the *newborn* infected, which are the individuals who get infected when they have not the infection, and the transitions between states of infection. For example, if an individual gets infected and is asymptomatic, it will be a newborn infection. If after a period of time it becomes symptomatic, this is a transition between states of infection.
To compute $\mathcal{R}_0$ we will use the subsystem of infected individuals, and linearize the system around the infection free steady state. Therefore we compute the Jacobian matrix and evaluate it at the DFE, which is denoted by J_{p_0}.
Secondly we need to decompose the J_{p_0} as follows :

$$J_{p_0} = \Sigma + T,$$

where T is the transmission matrix, describing the production of new infected individuals, and Σ is the transition matrix, which contains the coefficients of J_{p_0} corresponding to the transition between infected states. We introduce two definitions:

Definition 4.1. Let A be a matrix. We will say that (a_{ij}) is a positive matrix if and only if $a_{i,j} \geq 0, \forall i, j$ and we denote it by $A \geq 0$.

Definition 4.2. Let A be a matrix. We will say that (a_{ij}) is a positive-off-diagonal matrix if and only if $a_{i,j} \geq 0, \forall i \neq j$ and we denote it by $A \overset{d}{\geq} 0$.

The matrices T and Σ satisfy the following properties:

1. T is a positive matrix.
2. Σ is a positive-off-diagonal matrix.

We will show a brief explanation of the derivation of the Next generation matrix, $K = -T\Sigma^{-1}$, given with more detail in [10]. If we consider the system with reinfection turn off, we have the following system:

$$\dot{x} = \Sigma x, \tag{25}$$

a solution of the system will be $\psi(x) = e^{\Sigma t}\psi(0)$, so if we apply the reinfection to the solution and integrate it in time from zero to infinity, we get that:

$$K = \int_0^\infty T e^{\Sigma t}\psi(0) = -T\Sigma^{-1}. \tag{26}$$

Since $\psi(0)$ is the initial infected people and we suppose that it is equal to one and $-\Sigma^{-1}$ is a positive matrix, then $e^{\Sigma t}$ tends to zero when t tends to infinity.

The construction of the Next Generation Matrix has a biological meaning: $-(\Sigma^{-1})_{ij}$ is the expected time that an individual will stay in state i, assuming that it is in state j and T_{ij} is the rate at which individuals in state of infection j produce individuals at state at infection i. Consequently $(K_L)_{ij}$ corresponds to the expected number of new infected individuals starting in state i and caused by an individual in the state j. The definition of T and Σ does not determine uniquely the Next Generation Matrix $K = -T\Sigma^{-1}$ and consequently $\mathcal{R}_0$. In [8] they define the basic reproduction rate as $\mathcal{R}_0 = \rho(K)$, with $\rho(K) := sup_{\lambda_i \in \Lambda}\{|\lambda_i|\}$ the spectral radius of K, and Λ the set of all eigenvalues of K.

Since the computation of $\mathcal{R}_0$ depends on the construction of T and Σ, one of the inconveniences of this algorithm is the non-uniqueness of the decomposition $J = \Sigma + T$ and therefore $\mathcal{R}_0$. For instance, a transition between a latency state, where the individual is asymptomatic, and a infectious state does not involve a new infection, but rather a transition between states of infection. So in principal, these transitions will not be taken into account in T. In [8] they distinguish between the Next Generation matrix with Large domain, K_L, where more that the purely new infections are consider in the construction of T and the Next Generation Matrix K. They show that $\rho(K) = \rho(K_L)$.
An important result has been proved in [8], which states the following result: if $K = -T\Sigma^{-1}$ with $T \geq 0$ and $\Sigma \overset{d}{\geq} 0$ then $\text{sign}(r) = \text{sign}(1 - \mathcal{R}_0)$, where $r = s(T + \Sigma)$ is the Malthus reproduction parameter. We recall that if U is a square matrix then $s(U) = \sup\{\text{Re}(\lambda_i), \lambda_i \in \text{Spec}(U)\}$.
The stability at the DFE of the linearized system:

$$\frac{dx}{dt} = (T + \Sigma)x,$$

is given by the sign of the Malthusian parameter $r = s(T + \Sigma)$. Therefore it provides information of the stability of the linear system and of the local stability for the complete one.

Theorem 4.3. *Let T be a positive matrix and let Σ be a positive off-diagonal matrix with $s(\Sigma) < 0$ and $\mathcal{R}_0 := \rho(-T\Sigma^{-1})$. Consider $r := s(T + \Sigma)$. Then the following equality holds:*

$$\text{sign}(r) = \text{sign}(\mathcal{R}_0 - 1) \tag{27}$$

Here we can observe the relation between $\mathcal{R}_0$ being smaller and greater than one and the local stability of the DFE.

We will do an sketch of the proof (further detailed explanation is in [8]).

Theorem 4.4. *Let A be a positive-off-diagonal matrix. Then $s(A) < 0$ if and only if A is invertible and $-A^{-1}$ is a positive matrix.*

The proof of this theorem is in [10]. For the sake of completeness we present in this report an sketch of it.
First we will introduce some lemmas which hold under the following assumptions:

1. The matrix $(T + \Sigma)$ is a irreducible matrix,
2. $\mathcal{R}_0 > 0$.

Lemma 4.5. *If* $\mathcal{R} > 0$ *then* $s(\mathcal{R}_0^{-1}T + \Sigma) = 0$.

Now we construct a function $f : \mathbb{R} \to \mathbb{R}$, with $f(y) = s(y^{-1}T + \Sigma)$. The following statement holds:

Lemma 4.6. *if* $T + \Sigma$ *is an irreducible matrix then the function* f *is strictly monotonically decreasing.*

Now we prove the theorem with the two assumptions presented before.

Lemma 4.7. *If* $T + \Sigma$ *is irreducible and* $\mathcal{R}_0 > 0$ *then* $\text{sign}(r) = \text{sign}(\mathcal{R}_0 - 1)$.

Proof. We subdivide the proof into three different scenarios.

1. If $\mathcal{R}_0 > 1$, by lemma 4.6, $s(T + \Sigma) > s(\mathcal{R}_0^{-1}T + \Sigma)$ and since $s(\mathcal{R}_0^{-1}T + \Sigma) = 0$, by lemma 4.5, $s(T + \Sigma) > s(\mathcal{R}_0^{-1}T + \Sigma) = 0$ then $(T + \Sigma) > 0$.
2. If $\mathcal{R}_0 = 1$, by lemma 4.5, $s(T + \Sigma) = 0$.
3. If $\mathcal{R}_0 < 1$ then, by lemma 4.6, $s(T + \Sigma) < s(\mathcal{R}_0^{-1}T + \Sigma)$ and, by lemma 4.5, $s(\mathcal{R}_0^{-1}T + \Sigma) = 0$ hence $(T + \Sigma) < 0$.

□

Lemma 4.8. *If* $s(T + \Sigma) = 0$ *then* $\mathcal{R}_0 \geq 1$

Proof. By the arguments above it follows that $s(T + \Sigma)$ is an eigenvalue, and since we assume that $s(T+\Sigma) = 0$, then $T+\Sigma$ has eigenvalue 0. Let $u \neq 0$ be the corresponding eigenvector, i.e. $(T+\Sigma)u = 0$ and we define a vector $v \neq 0$ such that $v = \Sigma u$. Since Σ is an invertible matrix and $v \neq 0$, if we add $(T\Sigma^{-1})v$ to both side of the equation $v = \Sigma u$ after some calculations we get the following result: $(T\Sigma^{-1} + I)v = (T + \Sigma)u = 0$, so we get that $-T\Sigma^{-1}v = Iv = v$ and therefore 1 is an eigenvalue of $K_L = -T\Sigma^{-1}$. Consequently the spectral radius will be greater or equal to one. □

From this lemma we can prove a more restricted result.

Lemma 4.9. *If* $s(T + \Sigma) = 0$ *then* $\mathcal{R}_0 = 1$

Proof. We define a function of ϵ, namely $A(\epsilon) = T + \Sigma + 1\epsilon$, where we denote by 1 the matrix with all coefficients equal to one. Using the arguments of the proof of the lemma 4.6, explained in [8], we have that the function $\epsilon \to s(A(\epsilon))$ is monotonically increasing.
If we construct another function $\tilde{A}(\epsilon) = A(\epsilon) - s(A(2\epsilon))I$, since $\epsilon \to s(A(\epsilon))$ is a monotonically increasing function we have that

$$s(\tilde{A}(\epsilon)) = s(A(\epsilon)) - s(A(2\epsilon)) \leq 0. \tag{28}$$

It is clear that $\tilde{A}(\epsilon)$ tends to $T+\Sigma$ as ϵ tends to zero. Having that $s(\tilde{A}(\epsilon)) = (T+\epsilon 1)+(\Sigma - s(A(2\epsilon)I))$ we construct the function M as follows:

$$M(\epsilon) = -(T+\epsilon 1)(\Sigma - s(A(2\epsilon)I))^{-1}, \tag{29}$$

which tends to $K_L = -T\Sigma$ as ϵ tends to zero. By Lemma 4.8, $\mathcal{R}_0 = \rho(K_L) \geq 1$ then $\rho(M(\epsilon))$ should be positive for $\epsilon << 1$. Since $\tilde{A}(\epsilon)$ is irreducible by lemma 4.7 then $\text{sign}(s(\tilde{A}(\epsilon))) = \text{sign}(\rho(M(\epsilon)-1))$, using the inequality (28) we have that $\rho(M(\epsilon)) \leq 1$. Therefore, we have proved that $\mathcal{R}_0 = 1$. □

Proof of the theorem 4.3: By lemmas 4.9 and 4.5, with $\mathcal{R}_0 = 1$, we have that:

$$s(T+\Sigma) = 0 \iff \mathcal{R}_0 = 1. \tag{30}$$

By lemma 4.7, with $\epsilon << 1$, we conclude that:

$$s(T+\epsilon 1+\Sigma) < 0 \iff \rho(-(T+\epsilon 1)\Sigma^{-1}) < 1, \tag{31}$$

so when ϵ tends to zero we have that $s(T+\Sigma) < 0 \Rightarrow \mathcal{R}_0 \leq 1$ and that $\mathcal{R}_0 < 1 \Rightarrow s(T+\Sigma) \leq 0$. Since the equality (30) holds, we have that $s(T+\Sigma) < 0 \iff \mathcal{R}_0 < 1$. And we can conclude that $s(T+\Sigma) > 0 \iff \mathcal{R}_0 > 1$. So we have proved that :

$$\text{sign}(r) = \text{sign}(\mathcal{R}_0 - 1). \tag{32}$$

4.3 The Diekmann-Heesterbek algorithm, an example:

We present an example to give a better understanding of the algorithm:

Computation of $\mathcal{R}_0$ for COVID-19: In [14] it is shown a model for COVID-19 and a computation of $\mathcal{R}_0$ for this model. We have used a different approach for this computation. We take into account for the computation of $\mathcal{R}_0$ the equation related to the infected reported individuals, denoted by R in this case. The model used in [14] is the following:

$$\begin{aligned}
\frac{dS}{dt} &= -\tau S(t)(I(t)+U(t)) \\
\frac{dI}{dt} &= \tau S(t)(I(t)+U(t)) - \nu I(t) \\
\frac{dR}{dt} &= \nu_1 I(t) - \eta R(t) \\
\frac{dU}{dt} &= \nu_2 I(t) - \eta U(t)
\end{aligned} \tag{33}$$

where S denotes the susceptible individuals, I the infected asymptomatic individuals, R are the infected reported individuals with severe symptoms and U the unreported infected individuals with mild symptoms. An explanation of the parameters is given in table 2. First, we subdivide the system and take the equations which are related to the infected individuals, which are the following:

$$\begin{aligned}
\frac{dI}{dt} &= \tau S(t)(I(t)+U(t)) - \nu I(t) \\
\frac{dR}{dt} &= \nu_1 I(t) - \eta R(t) \\
\frac{dU}{dt} &= \nu_2 I(t) - \eta U(t)
\end{aligned} \tag{34}$$

Model Parameter	Interpretation
t_0	Time at which the epidemic started
S_0	Number of susceptible individuals at time t_0
I_0	Number of asymptomatic infectious individuals at time t_0
U_0	Number of unreported symptomatic infectious individuals at time t_0
τ	Transmission rate
$1/\nu$	Average time during which asymptomatic infectious are asymptomatic
f	Fraction of asymptomatic infectious become reported symptomatic
$\nu_1 = f\nu$	Rate at which asymptomatic infectious become reported symptomatic
$\nu_2 = (1-f)\nu$	Fraction of asymptomatic infectious become unreported symptomatic
$1/\eta$	Average time symptomatic infectious have symptoms

Table 2: List of parameters for the model given in [14].

Now we compute the Jacobian matrix for the subsystem:

$$J = \begin{pmatrix} \tau S - \nu & 0 & \tau S \\ \nu_1 & -\eta & 0 \\ \nu_2 & 0 & -\eta \end{pmatrix}, \tag{35}$$

and we evaluate J at the disease free steady state (DFE) $p_0 = (S_0, 0, 0, 0)$. We obtain the following matrix:

$$J = \begin{pmatrix} \tau S_0 - \nu & 0 & \tau S_0 \\ \nu_1 & -\eta & 0 \\ \nu_2 & 0 & -\eta \end{pmatrix}, \tag{36}$$

Now we split this matrix into T and Σ to compute the next generation matrix with large domain K_L,

$$T = \begin{pmatrix} \tau S_0 & 0 & \tau S_0 \\ \nu_1 & 0 & 0 \\ \nu_2 & 0 & 0 \end{pmatrix} \quad \Sigma = \begin{pmatrix} -\nu & 0 & 0 \\ 0 & -\eta & 0 \\ 0 & 0 & -\eta \end{pmatrix},$$

We compute the inverse of Σ, multiply it by $-T$, and we get:

$$K_L = \begin{pmatrix} \frac{\tau S_0}{\nu} & 0 & \frac{\tau S_0}{\nu} \\ \frac{\nu_1}{\nu} & 0 & 0 \\ \frac{\nu_2}{\nu} & 0 & 0 \end{pmatrix}. \tag{37}$$

We compute the eigenvalues of K_L: one eigenvalue is identically zero, $\lambda_1 = 0$, and two complex conjugate eigenvalues

$$\lambda_\pm = \frac{\tau S_0 \eta \pm \sqrt{\tau S_0 \eta(\tau S_0 \eta + 4\nu_2 \nu)}}{2\eta\nu}.$$

After some simplifications we get the following expression:

$$\lambda_\pm = 1 \pm \sqrt{1 + \frac{4\nu_2\nu}{\tau S_0 \eta}},$$

We can distinguish between three scenarios depending on the sign of the discriminant, $1 + \frac{4\nu_2\nu}{\tau S_0\eta}$:

1. The discriminant is equal to zero: we get one eigenvalue with multiplicity 2: $\frac{\tau S_0}{2\nu} = \frac{-2\nu_2}{\eta}$. Then the basic reproduction rate will be equal to:

$$\mathcal{R}_0 = \frac{\tau S_0}{2\nu}$$

2. The discriminant is greater than zero: we obtain two real eigenvalues: $\frac{\tau S_0}{2\nu} > \frac{-2\nu_2}{\eta}$. Then the basic reproduction rate will be equal to:

$$\mathcal{R}_0 = \frac{\tau S_0}{2\nu}(1 + \sqrt{1 + \frac{4\nu_2\nu}{\tau S_0 \eta}})$$

3. The discriminant is less than zero: we obtain two complex eigenvalues: $\frac{\tau S_0}{2\nu} < \frac{-2\nu_2}{\eta}$ and so

$$\mathcal{R}_0 = \frac{\tau S_0}{2\nu}\sqrt{2 + \frac{4\nu_2\nu}{\tau S_0 \eta}}$$

For the values of the parameters given in [14] we get that $\mathcal{R}_0 = 3.60$ which means that the steady state is unstable so it is a pandemic state.

A very useful tool to compute the basic reproduction rate is the algorithm developed by Diekmann and Heesterbek (the one presented in this section). However, there are other methods to compute $\mathcal{R}_0$. Some of then are more intuitive and "handmade". In the Appendix B of [1] it is presented a computation of $\mathcal{R}_0$ in this manner. Here we give a quick view of the process made in [1] to compute $\mathcal{R}_0$. First, they assume two conditions:

1. The system is "closed", in our equation (6) this means that $\beta_e = 0$. It assumes that there are no imported cases coming from other countries where malaria is present. The only possible way to get infected is from individuals who are in the population.

2. The carrying capacity is constant, $K = K_0$.

$\mathcal{R}_0$ is factorized as follows:

$$\mathcal{R}_0^2 = V_0 R \tag{38}$$

where V_0 is the vector capacity and $\mathcal{R}$ is the factor that depends on human related disease parameters. After some computations they obtained the following approximation for $\mathcal{R}_0$:

$$\mathcal{R}_0^{(b)} = a\sqrt{bc}\sqrt{\frac{Kd_L(f - \delta_M(1 + (\delta_L/d_L)))}{N\delta_M f}}\sqrt{\frac{1}{(\delta_H + r_0)\delta_M}}\left(\frac{n_P\gamma_P}{n_P\gamma_P + \delta_M}\right)^{\frac{n_P}{2}}\left(\frac{n_H\gamma_H}{n_H\gamma_H + r_0 + \delta_H}\right)^{\frac{n_H}{2}}, \tag{39}$$

As the authors observed this computation of $\mathcal{R}_0$ seems to be accurate since it takes into account the distributed delay introduced by the development of *Plasmodium* in the mosquito and the incubation phase of malaria in the human body.

5. Parameters to measure the epidemiology state apply to Malaria

5.1 Computation of $\mathcal{R}_0$ for the Malaria:

In this section we present the Diekmann and Heesterbek algorithm applied to our model.

First we construct the infectious subsystem, which is given by :

$$\begin{aligned}
\frac{dE}{dt} &= \beta S - \delta_H E - \gamma n_H E \\
\frac{dI}{dt} &= (1-\xi)\gamma n_H E - \eta\beta I + \nu C - rI - \delta_H I \\
\frac{dC}{dt} &= \xi\gamma n_H E + \eta\beta I - \nu C - \rho C - \delta_H C \\
\frac{dV}{dt} &= cayX - \gamma_P n_P V - \delta_M V \\
\frac{dW}{dt} &= \gamma_P n_P V - \delta_M W
\end{aligned} \tag{40}$$

We will assume that the system is "closed" so for equation (6), $\beta_e = 0$. The disease free point (DFE) for the system is of the type $p_0 = (S_0, 0, 0, 0, 0, L_0, X_0, 0, 0, 0)$, and the Jacobian Matrix is given by:

$$J = \begin{pmatrix}
-\delta_H - \gamma n_H & 0 & 0 & 0 & \frac{abS}{N} \\
(1-\xi)\gamma n_H & -\eta\frac{abW}{N} - fW - \delta_H & \nu & 0 & -\eta\frac{abI}{N} - fI + \frac{WIe^{aW/Nr_0}}{r_0}f^2 \\
\xi\gamma n_H & \eta\frac{abW}{N} & -(\nu+\rho+\delta_H) & 0 & \eta\frac{abI}{N} \\
0 & \frac{caX}{N} & \frac{caX}{N} & -\gamma_P n_P - \delta_M & 0 \\
0 & 0 & 0 & \gamma_P n_P & -\delta_M
\end{pmatrix}, \tag{41}$$

where $f = \frac{a}{N(e^{aW/Nr_0}-1)}$. Now we substitute the disease free steady state p_0 in J, as we can observe there will be some problems in the terms where f is involved, since when W tends to zero f goes to infinity. To avoid this inconvenient we need to approximate the components which are multiplied by f by the Taylor expansion and assume that $Y \leq c_y W$ with $c \in \mathbb{R}$ and is greater than zero.
There are three expressions that we would like to approximate by Taylor:

1. $\frac{aW}{N(e^{aW/Nr_0}-1)} \approx \frac{aW/N}{((aW/Nr_0+O(aW/Nr_0)^2))} = \frac{r_0}{1+O(aW/Nr_0)} \to r_0$ when $W \to 0$.

2. $\frac{a^2WIe^{aW/Nr_0}}{r_0(N(e^{aW/Nr_0}-1))^2} \approx \frac{a^2WI(aW/Nr_0+O(aW/Nr_0)^2)}{r_0N^2((aW/Nr_0+O(aW/Nr_0)^2))^2} = \frac{aI}{N}\frac{1}{1+O(aW/Nr_0)} \to \frac{aI}{N}$ when $W \to 0$.

3. $\frac{-aI}{N(e^{aW/Nr_0}-1)} \approx \frac{-aI}{N(aW/Nr_0+O(aW/Nr_0)^2)} = \frac{-Ir_0}{W}\frac{1}{1+O(aW/r_0)}$ and if we use that $Y \leq c_y W$ we get the following : $-c_y r_0 \frac{1}{1+O(aW/Nr_0)} \to -c_y r_0$ when $W \to 0$.

We substitute in J the approximations computed before and we get the following matrix:

$$J = \begin{pmatrix} -\delta_H - \gamma n_H & 0 & 0 & 0 & \frac{abS}{N} \\ (1-\xi)\gamma n_H & -\eta\frac{abW}{N} - r_0 - \delta_H & \nu & 0 & -\eta\frac{abI}{N} - c_y r_0 + \frac{aI}{N} \\ \xi\gamma n_H & \eta\frac{abW}{N} & -(\nu+\rho+\delta_H) & 0 & \eta\frac{abI}{N} \\ 0 & \frac{caX}{N} & \frac{caX}{N} & -\gamma_P n_P - \delta_M & 0 \\ 0 & 0 & 0 & \gamma_P n_P & -\delta_M \end{pmatrix}, \quad (42)$$

Then we evaluate it at p_0 and we get the following matrix:

$$J(p_0) = \begin{pmatrix} -\delta_H - \gamma n_H & 0 & 0 & 0 & ab \\ (1-\xi)\gamma n_H & -r_0 - \delta_H & \nu & 0 & -c_y r_0 \\ \xi\gamma n_H & 0 & -(\nu+\rho+\delta_H) & 0 & 0 \\ 0 & \frac{caX_0}{N} & \frac{caX_0}{N} & -\gamma_P n_P - \delta_M & 0 \\ 0 & 0 & 0 & \gamma_P n_P & -\delta_M \end{pmatrix}, \quad (43)$$

the next step in the algorithm is to split the matrix $J(p_0)$ into the transmission matrix (T):

$$T = \begin{pmatrix} 0 & 0 & 0 & 0 & ab \\ \gamma n_H & 0 & \nu & 0 & 0 \\ \xi\gamma n_H & 0 & 0 & 0 & 0 \\ 0 & \frac{caX_0}{N} & \frac{caX_0}{N} & 0 & 0 \\ 0 & 0 & 0 & \gamma_P n_P & 0 \end{pmatrix}, \quad (44)$$

and transition matrix (Σ):

$$\Sigma = \begin{pmatrix} -\delta_H - \gamma n_H & 0 & 0 & 0 & 0 \\ -\xi\gamma n_H & -r_0 - \delta_H & 0 & 0 & -c_y r_0 \\ 0 & 0 & -(\nu+\rho+\delta_H) & 0 & 0 \\ 0 & 0 & 0 & -\gamma_P n_P - \delta_M & 0 \\ 0 & 0 & 0 & 0 & -\delta_M \end{pmatrix}, \quad (45)$$

Therefore we get that the next generation matrix with large domain, K_L for (24), is given by:

$$K_L = \begin{pmatrix} 0 & 0 & 0 & 0 & \frac{ab}{\delta_M} \\ \frac{\gamma n_H}{\gamma n_H + \delta_H} & 0 & \frac{\nu}{\nu+\rho+\delta_H} & 0 & 0 \\ \frac{\xi\gamma n_H}{\gamma n_H + \delta_H} & 0 & 0 & 0 & 0 \\ -\frac{caX_0\xi\gamma n_H}{N(\gamma n_H+\delta_H)(r_0+\delta_H)} & \frac{caX_0}{N(r_0+\delta_H)} & \frac{caX_0}{N(\nu+\rho+\delta_H)} & 0 & -\frac{caX_0 c_y r_0}{N\delta_M(r_0+\delta_H)} \\ 0 & 0 & 0 & \frac{\gamma_P n_P}{\gamma_P n_P + \delta_M} & 0 \end{pmatrix}, \quad (46)$$

We compute the eigenvalues for this matrix and we get three equal to zero and two complex conjugate eigenvalues of form:

$$\lambda_{\pm} = \pm\sqrt{\frac{caX_0\gamma_P n_P}{(\gamma_P n_P + \delta_M)\delta_M}\frac{c_y r_0}{N(r_0+\delta_H)}}\,i \quad (47)$$

Therefore, the basic reproduction rate $\mathcal{R}_0$ is given by the modulus of the complex eigenvalue:

$$\mathcal{R}_0 = \sqrt{\frac{caX_0\gamma_P n_P}{(\gamma_P n_P + \delta_M)\delta_M}\frac{c_y r_0}{N(r_0+\delta_H)}} \quad (48)$$

where the first quotient is related to the mosquito and the second to the human component. Although the parameters γ_P and δ_M depends on the temperatures, i.e, depends on time, (10) and (11). Since $\mathcal{R}_0$ is computed at the initial time, when there is one infected individual, the parameters γ_P and δ_M are constant.

5.2 Effective Reproduction rate

After computing the Basic reproduction number $\mathcal{R}_0$ for our problem, a question arises: does the basic reproduction rate really measure the real infection grade of a disease at any time?.
Since the $\mathcal{R}_0$ does not depend on time, the answer is no. $\mathcal{R}_0$ measures the average number of secondary cases in a population where there is an infected individual and the rest of the population is susceptible.
In reality a whole population is rarely susceptible to a disease. For example some individuals could be immune due to a prior infection which produced a temporary immunity. Therefore not all individuals could get infected, so the susceptible individuals are not the whole population. Therefore, the average number of cases per infectious case will be smaller than the basic reproduction rate. For this reason we need a measure which depends on time and takes into account that the number of susceptible individuals is a part of the whole population. This is called the *effective reproduction number*.

The effective reproduction number, $\mathcal{R}_t$, is the average number of secondary cases produced by a infected individual at time t in a population where there are susceptible and non susceptible individuals. It is computed as follows:

$$\mathcal{R}_t = \mathcal{R}_0 s(t), \tag{49}$$

where $s(t)$ is the fraction of the population which is susceptible to the disease at time t.
These past months in press, during the recently COVID-19 crisis, the term basic reproduction rate has been used wrongly when in fact they meant effective reproduction rate $\mathcal{R}_t$.

5.3 Deaths rates

In the previous section we have presented, R_t, a rate to measure the infection grade of a disease, crucial when there is a pandemic. However, there are other relevant rates, for example, those which measure the mortality produced by the disease.
One of the first questions that one asks when there is a pandemic is, if someone gets infected, how likely is that person to die?. This is a simple but hard to answer question because mortality rates rely on the information about the confirmed cases and the number of deaths. As we have experienced with COVID-19 this data is not trustworthy and also some people who are sick and soon will die.
Due to these two facts it is extremely complicated to compute accurately the risk of death. In addition in the context of Malaria in Kenya, the health care system is weaker than in the Western World and the level of poverty is higher. These are two key factors that increase the uncertainty in the data.
There are many indicators to measure the risk of dying. We will focus on two of them, the *Case Fatality Rate* or CFR and the *Crude Mortality Rate*.

The case fatality rate (CFR): The case fatality rate is one of the most commonly used rate to measure the risk of death. It is also called the "Case fatality risk" or "Case fatality ratio".
The CFR requires an easy calculation. It is the number of people who have died divided by the number of total people who have been diagnosed with the disease:

$$\text{Case fatality rates} = \frac{\text{Number of deaths from the disease}}{\text{Number of diagnosed cases from the disease}} \cdot 100. \tag{50}$$

Note that this is a ratio over the number of confirmed cases, so not over the total number of people who have got the disease. As we have experienced with COVID-19, the number of diagnosed people in Spain is

related to the people working in the health care system or the people who has severe symptoms and therefore they have gone to the hospital to receive clinical treatment. Since many people with weak symptoms or asymptomatic will not be included, this rate does not give the true risk of death. Consequently the CFR does not measure the true mortality risk.
For example, in a population of 500 individuals, 100 are infected by the disease, and 30% of these infected individuals are asymptomatic and consequently have not been diagnosed, and 10 people have died from the disease. We will have that the CFR = 14,28 % when in real it would be 10%, if all the asymptomatic cases had been diagnosed. This is a vital difference when we talk about the death risk of a disease.

Another important ratio to measure the death risk is the crude mortality rate:

The crude mortality rate (CMR): This rate is another simple measure, also called the crude death rate.
The difference with the case mortality rate is that, instead of dividing by the number of diagnosed cases, it is divided by the total number of susceptible individuals, i.e., the total size of the population:

$$\text{Crude mortality rate} = \frac{\text{Number of deaths from the disease}}{\text{Size of the population}} \cdot 100 \tag{51}$$

It is easy to observe that the crude mortality rate will be, in general, much smaller than the case mortality rate, since the number of diagnosed case is often much smaller than the size of the infected population, even for the most infectious diseases. For example, this happens with COVID-19 which is a highly contagious disease.
In the example given before the crude mortality rate will be 2%, a small amount compared to 14,28%. Even if there is a considerable difference between these two rates, they are often confused. A common example is the Spanish flu in 1918 where Johnson and Mueller confused the crude mortality rate with the case mortality rate in [13]. The pandemic killed around 50 million people, which is a 2.7% of the population of that time, and they used this amount as the case mortality rate. However, the case mortality rate was in fact much higher.
To answer the question, if a person is infected how likely is s/he to die?, None of the two ratios explained before could accurately answer this question. A rate which will answer with more accuracy this question will be the *Infection fatality rate*:

The infection fatality rate (IFR): It is defined as:

$$\text{Infection fatality rate} = \frac{\text{Number of deaths from the disease}}{\text{Number infected people}} \cdot 100, \tag{52}$$

This would be the rate which will measure the death risk of a sickness with more accuracy. However in reality we cannot know how many people have got infected by the disease, since there are only a part of this group which will be diagnosed. We can estimate the total number of cases, as we have done with for the case of Malaria before. But this will not produce an accurate infection fatality rate value.
For the example given for the other two rates, if we have 100 people infected and 10 deaths the infection fatality rate will be of 10%.

6. Conclusions and further studies

Even if not generally acknowledged, Malaria was an issue in the Mediterranean in the past. Historical records indicate that malaria was endemic from the Middle ages until the 1950s, when some policies where implemented to stop the epidemic. One of the most effective was the use of the chemical DDT (Dichlorodiphenyltrichloroethane). There have been many studies about the disease in the past and its social impact ([22],[19]).

Because of the tragic events of these last months and the fact that Malaria was present in the Mediterranean before, the following question arises: how likely it is that another malaria epidemic occurs in the Mediterranean? Could be this a feasible consequence of global warming?.

Malaria is one of the most widely-spread diseases in the world, causing thousands of deaths per year, mostly in sub-Saharan Africa, like in Kenya. However, the globalization and the increase of temperatures due to climate change have worried epidemiologists about the increase of malaria in Europe.

In the last few years an increase in malaria cases has been reported in the Mediterranean countries. Most of them are imported cases, which means that an individual has got the disease in an endemic country and travelled back to Europe [17]. This growth is probably supported by the increasing number of international travels to countries where malaria is endemic. In [24] there is a full report about the malaria cases in Europe from 2014 to 2018, with a distinction between imported and born cases. In [24] we can observe an increasing trend for Spain, going from 688 cases in 2014 to 851 in 2018.

For these reasons, we believe that studying the behaviour of malaria in the European Mediterranean can be of high interest. We have repeated the analysis with model (24) but now for malaria in the Mediterranean, keeping the same values for the parameters but adapting the climate data. To fix an example, we have taken this data, temperatures and rainfall, from a village, Agost, in Alicante which is located in the countryside of the region and with an economy based on agriculture. This data is from January to December of 2018 given in [25].

In fig. 18 a graph of the average temperatures in this region is shown. We can observe there is a maximum in the 216th day, corresponding to the 5th of August, with an average temperature of 29.03 Celsius degrees. The minimum is at day 49 (19th of February), where the average temperature reaches 10.03 degrees Celsius. As expected, average temperatures are higher during the summer.

Figure 18 displays the rainfall in mm during the same period as the temperatures. We can observe that the amount of rain is higher during the rainy seasons, from February to May and from September to November.

Now we would like to know what would happen if a small part of the population become infected. We use the climate data presented before for these simulations. The initial conditions are as follows: a total human population of 5000 individuals, which is approximately the population of Agost, with 99% of the population susceptible and the rest infected, corresponding to 50 individuals. We also assume that there are no recovered individuals. For the mosquito population we followed the same logic, taking a total population of 1000 adult mosquitoes where 99% are non infected mosquitoes and the rest are infected. For simplicity we use the value of the parameters presented in table 1.

Figure 20 shows the simulations related to the human population over a year. As we can observe, there is no increase of the infected individuals until approximately the day 150, which corresponds to the beginning of May. This is related to an increase on the average temperature, exceeding 20°. Between day 150 and 200 the susceptible individuals decrease until a relative minimum is reached, and at this point around the 80% of the population is infected or has been infected. After this increase on the infected individuals there

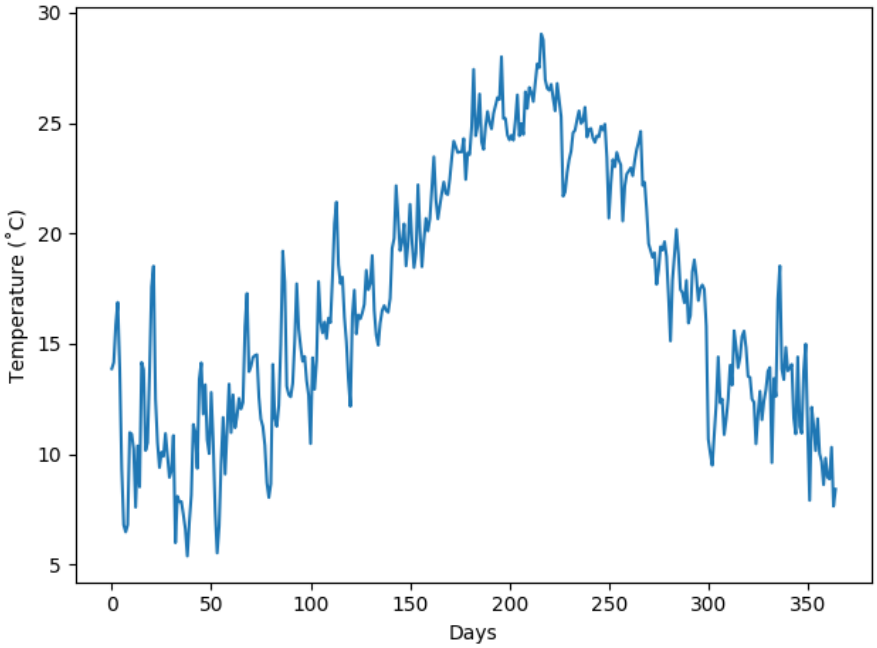

Figure 18: Average temperatures from 1st January to 31st December of 2018 in Agost, Alicante. Measured in degrees Celsius.

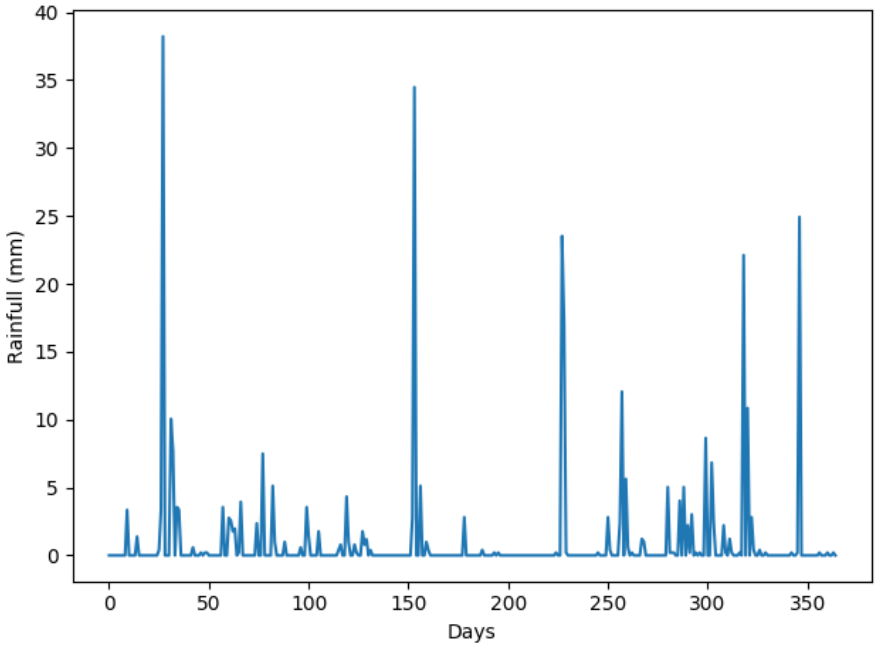

Figure 19: Rainfall from 1st January to 31st December of 2018 in Agost, Alicante. Measured in mm.

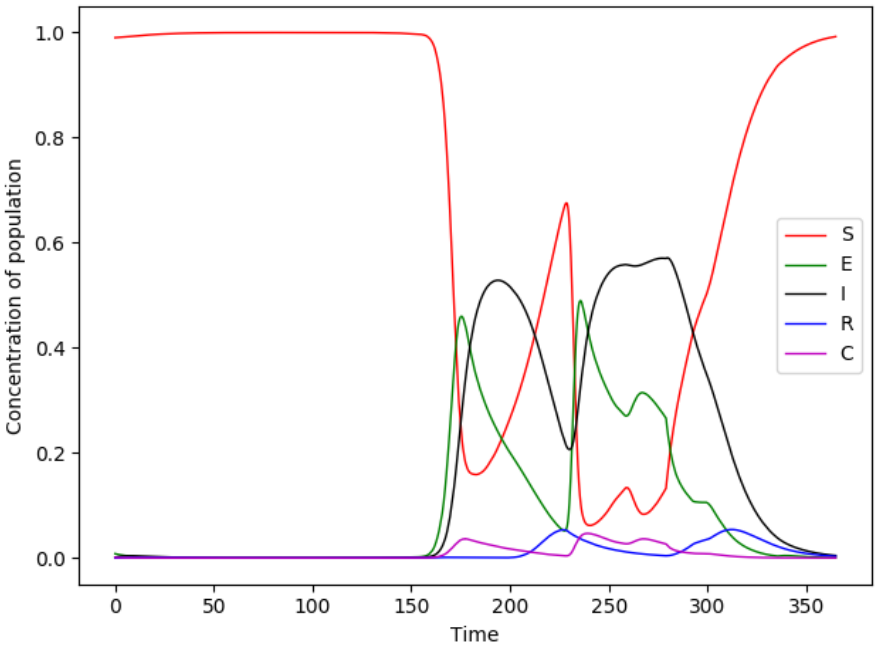

Figure 20: Numerical simulations of the model for the SEIR population normalized by the total population for the Mediterranean case.

are some fluctuations until around the 279 day where the susceptible individuals increase reaching almost the total population and infected individuals get closer to zero. Figure 18 shows how this is related to the decrease in the temperatures below the 20°.

A similar behaviour can be observed for the adult mosquito population. Figure 22 displays the adult mosquito population, note that between days 150 and 200 there is a decrease in the non infected population and a increase in the infected individual. This behaviour is expected since the development rate of the Plasmodium parasite increases with temperature, as it is shown in fig. 4.
After some fluctuations around the 300th day, the total adult mosquito population starts to decrease almost reaching extinction while the larvae continue to fluctuate reaching a relative maximum around the 350th day. This causes that even if the adult population is close to zero in a period of time, it increases due to a large amount of larvae, as we can observe in fig. 23.

An interesting remark is that even with a really small part of the population infected, as we have assumed for our simulations, the climate conditions of the Mediterranean could trigger an outbreak of malaria during a summer period.
If we compare the two cases studied in this project, the one related to malaria in Kenya and the basic study for the Mediterranean, we can see that in Kenya the epidemic is stronger since it is an endemic country and in the case of the Mediterranean the cases of malaria are mostly imported cases. However, as we have said at the beginning of section 3, the malaria was eradicated from Kenya Highlands and has returned back. Some researches believe that it is due to subtle changes in the region's climate. Since the number

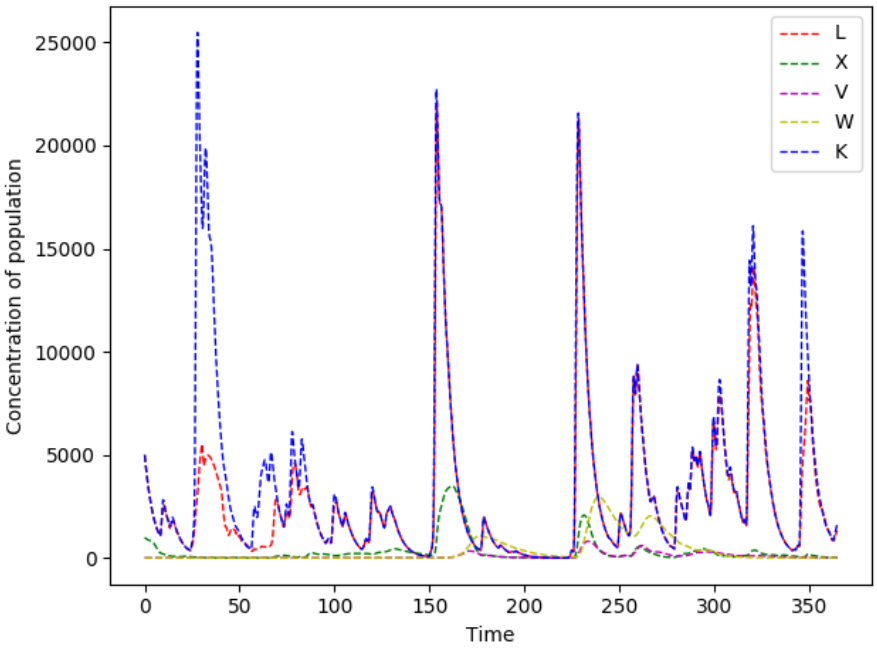

Figure 21: Numerical simulations of the model for the mosquito population and its carrying capacity for the Mediterranean case.

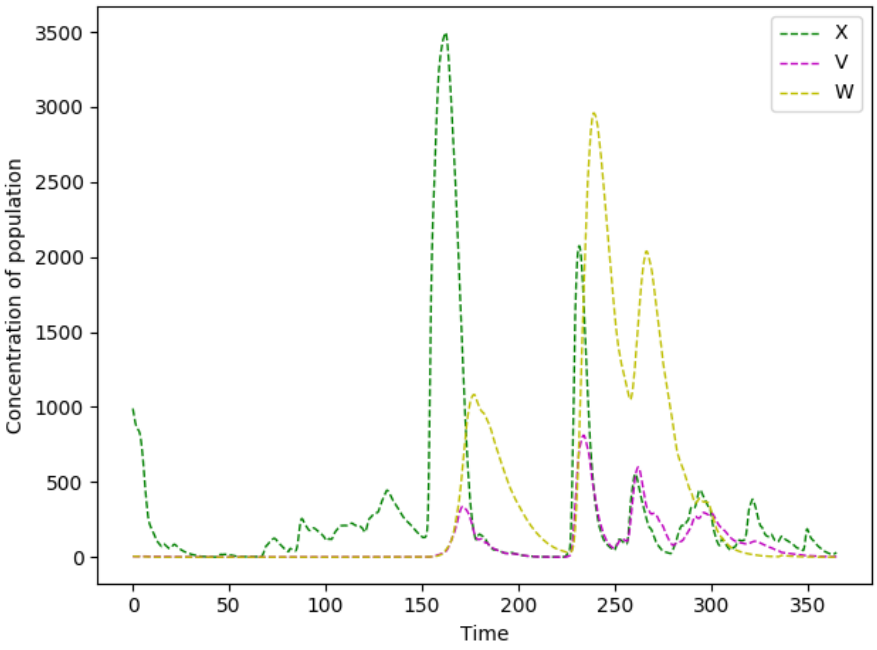

Figure 22: Numerical simulations of the model for the mosquito adult population for the Mediterranean case.

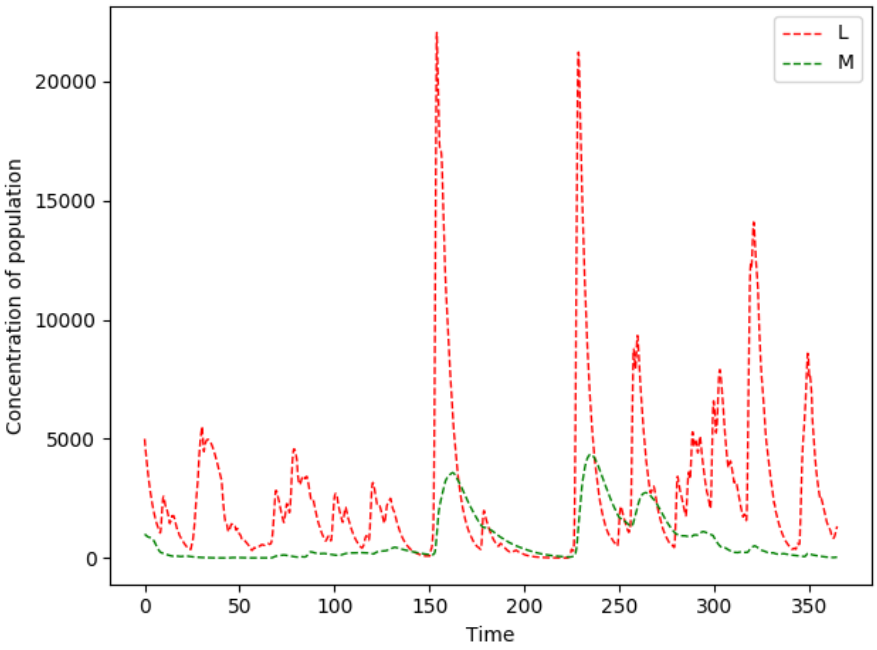

Figure 23: Numerical simulations of the model for the mosquito adult population, M, and the larvae, L, for the Mediterranean case over one year.

of mosquito vector is increasing in the Mediterranean, it would be interesting, as a further work, to study the effect of climate change on the malaria in the Mediterranean and to create a more specific model for this particular problem.

During this work I got into epidemiology, a field that I had no knowledge of before. In particular I have learnt about vector borne disease and how to model them.
First, I started with the simplest one, the SIR model, which is a compartmental model, i.e., it distributes the population in different compartments depending on the infectious states. After that, I studied more complex models which are variations of the SIR models, such as the one presented in this work. Since these are systems of ODE's that do not have an analytical solution I applied numerical methods to solve them. For this purpose I programmed in C, a programming language which I have not used before. I have also learnt more about non autonomous systems since during my degrees studies I was focused on autonomous systems. Due to the fact that everything gets more complicated when some parameters of the system depend on time, I have learnt how to study the system with a different approach.
In the other hand I have developed skills to work with models used in epidemiology dealing with different rates, like the basic reproduction rate, to measure if it is likely an outbreak of the disease.

References

[1] Alonso, David and Bouma, Menno and Pascual, Mercedes. *Epidemic malaria and warmer temperatures in recent decades in an East African highland. Proceedings.*, Biological sciences / The Royal Society. 278. 1661-9.

[2] Afrane YA, Lawson BW, Githeko AK, Yan G. *Effects of microclimatic changes caused by land use and land cover on duration of gonotrophic cycles of Anopheles gambiae (Diptera: Culicidae) in western Kenya highlands.* J Med Entomol. 2005;42(6):974-980. doi:10.1093/jmedent/42.6.974

[3] Alsop Z. *Malaria returns to Kenya's highlands as temperatures rise.* Lancet. 2007;370(9591):925-926. doi:10.1016/S0140-6736(07)61428-7

[4] Bacaër N. (2011) Ross and malaria (1911). *In: A Short History of Mathematical Population Dynamics.* Springer, London. https://doi.org/10.1007/978-0-85729-115-8˙12

[5] Bayoh, Nabie and Lindsay, Steve. (2004). *Temperature-related duration of aquatic stages of the Afrotropical malaria vector mosquito Anopheles gambiae in the laboratory.* Medical and veterinary entomology. 18. 174-9. 10.1111/j.0269-283X.2004.00495.x.

[6] Brauer, Fred and Driessche, P and Wu, Jianhong. (2008). Lecture Notes in Mathematical Epidemiology.

[7] B. Charlet, J. Lévine, R. Marino. On dynamic feedback linearization, *System and Control Letters* **13** (1989), 143–151.

[8] Diekmann O, Heesterbeek JA, Roberts MG. *The construction of next-generation matrices for compartmental epidemic models.* J R Soc Interface. 2010;7(47):873–885. doi:10.1098/rsif.2009.0386

[9] Diekmann, O., Heesterbeek, J.A.P. Metz, J.A.J. *On the definition and the computation of the basic reproduction ratio R 0 in models for infectious diseases in heterogeneous populations.* J. Math. Biol. 28, 365–382 (1990).

[10] Diekmann, O. Heesterbeek, J.A.P.. (2000). *Mathematical Epidemiology of Infectious Diseases: Model Building, Analysis and Interpretation.* Wiley Series in Mathematical and Computational Biology, Chichester, Wiley.

[11] Dietz, Klaus. (1993). *The Estimation of the Basic Reproduction Number for Infectious Diseases.* Statistical methods in medical research. 2. 23-41. 10.1177/096228029300200103.

[12] Hay, S. I., Cox, J., Rogers, D. J., Randolph, S. E., Stern, D. I., Shanks, G. D., Myers, M. F., Snow, R. W. (2002). *Climate change and the resurgence of malaria in the East African highlands.* Nature, 415(6874), 905–909. https://doi.org/10.1038/415905a

[13] Johnson NP, Mueller J. *Updating the accounts: global mortality of the 1918-1920 "Spanish" influenza pandemic.* Bull Hist Med. 2002;76(1):105-115. doi:10.1353/bhm.2002.0022

[14] Liu, Zhihua Magal, Pierre Seydi, Ousmane Webb , Glenn. (2020). *Understanding Unreported Cases in the COVID-19 Epidemic Outbreak in Wuhan, China, and the Importance of Major Public Health Interventions.* Biology. 9. 50. 10.3390/biology9030050.

[15] Macdonald G. *The analysis of equilibrium in malaria.* Tropical Diseases Bulletin. 1952 Sep;49(9):813-829.

[16] MacDonald, G, World Health Organization. Malaria Section Conference on Malaria in Africa (1955 : Lagos, Nigeria). (1955).*Epidemiological basis of malaria control* by G. MacDonald. World Health Organization. https://apps.who.int/iris/handle/10665/64382

[17] Odolini, S., Gautret, P., Parola, P. (2012).*Epidemiology of imported malaria in the mediterranean region.* Mediterranean journal of hematology and infectious diseases, 4(1), e2012031. https://doi.org/10.4084/MJHID.2012.031

[18] Richard S. Varga. *Matrix Iterative Analysis.* Nonnegative matrices, 35-39 (2000).

[19] Sallares, R., Bouwman, A., Anderung, C. (2004).*The Spread of Malaria to Southern Europe in Antiquity: New Approaches to Old Problems.* Medical History, 48(3), 311-328. doi:10.1017/S0025727300007651

[20] Smith C.E.G. *Factors in the transmission of virus infections from animals to man.* Scientific basis of Medicine. Ann.Rev.1964. 125-150.

[21] W. O. Kermack and A. G. McKendrick. *A contribution to the mathematical theory of epidemics.* , Proceedings of the Royal Society of London Series A, 115:700–721, 1927.

[22] University of Zurich. (2017, July 27). *Malaria already endemic in the Mediterranean by the Roman period.* ScienceDaily. Retrieved June 12, 2020

[23] WHO, World map of Malaria cases. Available at `https://www.who.int/malaria/areas/elimination/e2020/en/`(accessed on 20th May, 2020)

[24] *European Centre for Disease Prevention and Control.* Malaria. In: ECDC. Annual epidemiological report for 2018. Stockholm: ECDC; 2020. Available at `https://www.ecdc.europa.eu/sites/default/files/documents/malaria-annual-epidemiological-report-2018.pdf` (accessed on 20th May, 2020)

[25] *Instituto valenciano de investigaciones agrarias.* . Available at `http://riegos.ivia.es/` (accessed on 23th May, 2020)

A. Interpolation method: Splines

One key component on the model is the temperature and rainfall data, since the temperatures and rainfall are discrete values, sometimes given by days and in other cases monthly. We need to interpolate the data to have a continuous function, to do that we have used the interpolation method called cubics spline, which use the method of moments.
A spline of order k in an interval $[a, b]$ is a function which satisfies the following conditions:

1. S has continuous derivatives until order $k - 1$.
2. S is a polynomial piecewise function of order k.

In this work we use spline of order 3 which are called cubic splines.
If we have a set of points $\{x_0, x_1, ..., x_n\}$ and the value of the function evaluated in this set of points $\{f(x_1) = y_1, f(x_2) = y_2, ..., f(x_n) = y_n\}$. The associated cubic spline should satisfy that:

1. $S(x_i) = y_i$, $\forall x \in \{1, 2, ..., n\}$.
2. S is a polynomial of degree 3 defined for each interval $\{x_i, x_{i+1}\}$.
3. $S \in \mathcal{C}^2$.

Imposing some conditions to S, we get the following expression:

$$S_i(x) = A_i + B_i(x - x_i) + M_i\frac{(x - x_i)^2}{2} + \frac{M_{i+1} - M_i}{h_i}\frac{(x - x_i)^3}{6}, \tag{53}$$

where $h_i = x_{i+1} - x_i$, $A_i = f(x_i)$, $d_{i+1} = 6\left(\frac{f(x_{i+2})-f(x_{i+1})}{h_{i+1}} - \frac{f(x_{i+1})-f(x_i)}{h_i}\right)$ and we need to solve the following tridiagonal system of equations to obtain the values of M_i:

$$T\begin{bmatrix} M_1 \\ . \\ . \\ . \\ M_{n-1} \end{bmatrix} = \begin{bmatrix} d_1 \\ . \\ . \\ . \\ d_{n-1} \end{bmatrix}, \tag{54}$$

where T is defined as follows:

$$T = \begin{bmatrix} 2(h_0 + h_1) & h_1 & & & & \\ h_1 & 2(h_0 + h_1) & h_2 & & & \\ & . & . & . & & \\ & & . & . & . & \\ & & & h_{n-2} & 2(h_{n-2} + h_{n-1}) & \end{bmatrix}, \tag{55}$$

and

$$B_i = \frac{f(x_{i+1}) - f(x_i)}{h_i} - (M_{i+1} - M_i)\frac{h_i}{6} - M_i\frac{h_i}{2}.$$

B. Definitions, Lemmas and Theorems

Definition B.1. A $n \times n$ matrix A, is called an irreducible matrix if there is no permutation of coordinates such that:

$$P^T A P = \begin{bmatrix} A_{11} & A_{12} \\ 0 & A_{22} \end{bmatrix}, \tag{56}$$

where P is a $n \times n$ permutation matrix.

Theorem B.2. Perron-Frobenius Theorem for irreducible matrix
If $A = (a_{i,j})$ is $n \times n$ nonnegative and irreducible matrix, the following statements holds:

1. *One of its eigenvalues is positive and greater than or equal, in absolute value, to all other eigenvalues. This eigenvalue is called the "the dominant eigenvalue" or Perron-Frobenius eigenvalue of the matrix.*
2. *There is a positive eigenvector corresponding to this eigenvalue.*
3. *The spectral radius $\rho(A)$ is equal to this eigenvalue and it satisfies the following:*

$$\min_i \sum_j a_{i,j} \leq \rho(A) \leq \max_i \sum_j a_{i,j}$$

A proof of the Perron-Frobenius theorem could be found in [18].